

Chapter 1

Wakes and Impedances

1.1 Wake Fields

A positively charged particle at rest has static electric field going out radially in all directions. In motion with velocity v , magnetic field is generated. As the particle velocity approaches c , the velocity of light, the electric and magnetic fields are pancake-like, the electric field is radial and magnetic field azimuthal (the Liénard–Wiechert fields [1]) with an open angle of about $1/\gamma$, where $\gamma = (1 - v^2/c^2)^{-1/2}$. It is interesting to point out that no matter how far away, this pancake is always perpendicular to the path of motion. In other words, the fields move with the test particle without any lagging behind as illustrated in Fig. 1.1. Such a field pattern does not necessarily violate causality because it is a steady-state solution, which may require a long time to establish.

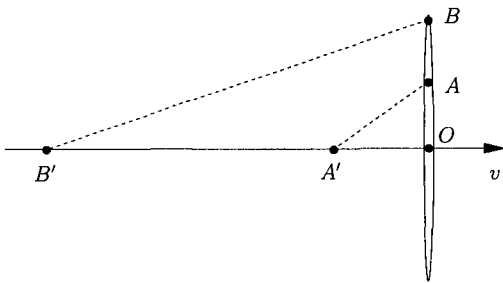


Fig. 1.1 Schematic drawing of pancake electromagnetic fields emitted by an ultra-relativistic particle traveling with velocity v . The pancake is always perpendicular to the path of the particle and travels in pace with the particle no matter how far away the fields are from the particle. There is no violation of causality because fields at points A and B come from the particle at different locations, respectively, from A' at a time OA'/v ago and from B' at a time OB'/v ago.

When placed inside a perfectly conducting beam pipe, the pancake of fields is trimmed by the beam pipe. A ring of negative charges will be formed on the walls of the beam pipe where the electric field ends, and these image charges will travel at the same pace with the particle, creating the so-called *image current*. If the

wall of the beam pipe is not perfectly conducting or contains discontinuities, the movement of the image charges will be slowed down, thus leaving electromagnetic fields behind. For example, upon coming across a cavity, the image current will flow into the walls of the cavity, exciting fields trapped inside the cavity. These fields left behind by the particle are called *wake fields*, which are important because they influence the motion of the particles that follow.

In addition to the wake fields, the electromagnetic fields experienced by the beam particle also consist of the external fields from the guiding and focusing magnets, rf cavities, etc. The electric field \vec{E} and magnetic flux density \vec{B} can be written as

$$(\vec{E}, \vec{B})_{\text{seen by particles}} = (\vec{E}, \vec{B})_{\text{external, from magnets, rf, etc.}} + (\vec{E}, \vec{B})_{\text{wake fields}}, \quad (1.1)$$

where

$$(\vec{E}, \vec{B})_{\text{wake fields}} \begin{cases} \propto \text{beam intensity,} \\ \ll (\vec{E}, \vec{B})_{\text{external.}} \end{cases}$$

Note that the last restriction, which is certainly not true in plasma physics, allows the wake fields inside the vacuum chamber to be treated as perturbation. This perturbation, however, will break down when potential-well distortion is large. In that case, the potential-well distortion has to be included into the non-perturbative part. What we need to compute are the wake fields at a distance z behind the source particle and their effects on the test or witness particles that make up the beam. The computation of the wake fields is nontrivial. Two approximations are therefore introduced.

1.1.1 Two Approximations

At high energies, the particle beam is rigid and the following two approximations apply:*

(1) **The rigid-beam approximation**, which says that the beam traverses the discontinuities of the vacuum chamber rigidly and the wake-field perturbation does not affect the motion of the beam during the traversal of the discontinuities. This is a good approximation even in the presence of synchrotron oscillations, because the longitudinal distance between two beam particles changes negligibly in a revolution turn relative to the bunch length. This implies that the distance z of the test particle behind some source particle as shown in Fig. 1.2 does not change.

*This approach to the Panofsky-Wenzel Theorem was first presented by A. W. Chao at the OCPA Accelerator School, Hsinchu, Taiwan, August 3-12, 1998.

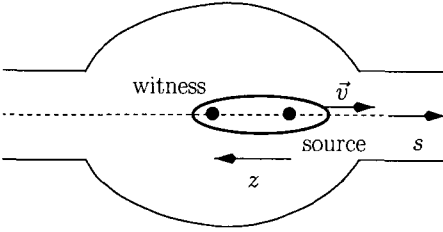


Fig. 1.2 Schematic drawing of a witness particle at a distance z behind some source particle in a beam. Both particles are traveling along the direction s with velocity \vec{v} .

(2) **The impulse approximation.** Although the test particle carrying a charge q sees a wake force \vec{F} coming from (\vec{E}, \vec{B}) , what it cares for is the impulse

$$\Delta\vec{p} = \int_{-\infty}^{\infty} dt \vec{F} = \int_{-\infty}^{\infty} dt q(\vec{E} + \vec{v} \times \vec{B}), \quad (1.2)$$

as it completes the traversal through the discontinuities at its fixed velocity \vec{v} . Note that MKS units have been used in Eq. (1.2) and will be adopted throughout the rest of the book. We will therefore be coming across the electric permittivity of free space $\epsilon_0 = 10^7/(4\pi c^2)$ farads/m and the magnetic permeability of free space $\mu_0 = 4\pi \times 10^{-7}$ henry/m. These two quantities are related to the free-space impedance Z_0 and velocity of light c by

$$Z_0 = \sqrt{\frac{\mu_0}{\epsilon_0}} = 2.99792458 \times 40\pi = 376.730313 \text{ Ohms}, \quad (1.3)$$

$$c = \frac{1}{\sqrt{\mu_0\epsilon_0}} = 2.99792458 \times 10^8 \text{ m/s}. \quad (1.4)$$

Both \vec{E} , \vec{B} and \vec{F} are difficult to compute even at high beam energies. However, the impulse $\Delta\vec{p}$ has great simplifying properties through the Panofsky–Wenzel theorem, which forms the basis of wake potentials and impedances.

1.1.2 Panofsky–Wenzel Theorem

Maxwell equations for a particle in the beam are

$$\left\{ \begin{array}{ll} \vec{\nabla} \cdot \vec{E} = \frac{\rho}{\epsilon_0} & \text{Gauss's law for electric charge,} \\ \vec{\nabla} \times \vec{B} - \frac{1}{c^2} \frac{\partial \vec{E}}{\partial t} = \mu_0 \beta c \rho \hat{s} & \text{Ampere's law,} \\ \vec{\nabla} \cdot \vec{B} = 0 & \text{Gauss's law for magnetic charge,} \\ \vec{\nabla} \times \vec{E} + \frac{\partial \vec{B}}{\partial t} = 0 & \text{Faraday's \& Lenz law.} \end{array} \right. \quad (1.5)$$

$$\begin{aligned}\vec{\nabla} \times \Delta \vec{p} &= -q \int_{-\infty}^{\infty} dt \left[\left(\frac{\partial}{\partial t} + \beta c \frac{\partial}{\partial s} \right) \vec{B}(x, y, s, t) \right]_{s=z+\beta ct} \\ &= -q \int_{-\infty}^{\infty} dt \frac{d\vec{B}}{dt} = -q \vec{B}(x, y, z+\beta ct, t) \Big|_{t=-\infty}^{\infty} = 0,\end{aligned}\quad (1.10)$$

which is the Panofsky-Wenzel theorem. It is important to note that so far no boundary conditions have been imposed. The Panofsky-Wenzel theorem is valid for any boundaries! The only needed inputs are the two approximations: the rigid-bunch approximation and the impulse approximation. The Panofsky-Wenzel theorem even does not require $\beta = 1$. It just requires $\beta \approx 1$ so that β can remain constant. Thus, the Panofsky-Wenzel theorem is very general.

The Panofsky-Wenzel theorem can be decomposed into a component parallel to \hat{s} and another perpendicular to \hat{s} . The decomposition is obtained by taking dot product and cross product of \hat{s} with Eq. (1.10):

$$\vec{\nabla} \cdot (\hat{s} \times \Delta \vec{p}) = 0, \quad (1.11)$$

$$\frac{\partial}{\partial z} \Delta \vec{p}_{\perp} = \vec{\nabla}_{\perp} \Delta p_s. \quad (1.12)$$

Equation (1.11) says something about the transverse components of $\Delta \vec{p}$, which becomes, in Cartesian coordinates,

$$\frac{\partial \Delta p_x}{\partial y} = \frac{\partial \Delta p_y}{\partial x}. \quad (1.13)$$

On the other hand, Eq. (1.12) relates $\Delta \vec{p}_{\perp}$ and $\Delta \vec{p}_s$, that the transverse gradient of the longitudinal impulse is equal to the longitudinal gradient of the transverse impulse. Thus, the Panofsky-Wenzel theorem strongly constraints the components of $\Delta \vec{p}$.

There is an important supplement to the Panofsky-Wenzel theorem, which states:

$$\beta = 1 \longrightarrow \vec{\nabla}_{\perp} \cdot \Delta \vec{p}_{\perp} = 0. \quad (1.14)$$

Proof:

$$\begin{aligned}\vec{\nabla} \cdot \Delta \vec{p} &= \int_{-\infty}^{\infty} dt \left[\vec{\nabla} \cdot \vec{F}(x, y, s, t) \right]_{s=z+ct} = -\frac{q}{c} \int_{-\infty}^{\infty} dt \left[\frac{\partial E_s}{\partial t} \right]_{s=z+ct} \\ &= q \int_{-\infty}^{\infty} dt \left[\frac{\partial E_s}{\partial s} \right]_{s=z+ct} = \frac{\partial}{\partial z} \Delta p_s,\end{aligned}$$

where we have used the fact that the longitudinal component of the wake force is independent of the magnetic flux density. For the second last step, use has been made of

$$\frac{\partial}{\partial t} E_s(s, t) = \frac{d}{dt} E_s(s, t) - \frac{ds}{dt} \frac{\partial}{\partial s} E_s(s, t). \quad (1.15)$$

It is important to note that $4\pi q\rho/\gamma^2$, the space-charge term of $\vec{\nabla} \cdot \vec{F}$ in Eq. (1.7) has been omitted because $\beta = 1$.

1.1.3 Cylindrically Symmetric Chamber

When the beam of cylindrical cross section is inside a cylindrically symmetric vacuum chamber, naturally cylindrical coordinates will be used. Some differential operators in the cylindrical coordinates are listed in Table 1.1. The Panofsky–Wenzel theorem, Eq. (1.10), and the supplemental theorem, Eq. (1.14), are rewritten as [3]

$$\left\{ \begin{array}{l} \frac{\partial}{\partial r} (r\Delta p_\theta) = \frac{\partial}{\partial \theta} \Delta p_r, \\ \frac{\partial}{\partial z} \Delta p_r = \frac{\partial}{\partial r} \Delta p_s, \\ \frac{\partial}{\partial z} \Delta p_\theta = \frac{1}{r} \frac{\partial}{\partial \theta} \Delta p_s, \\ \frac{\partial}{\partial r} (r\Delta p_r) = -\frac{\partial}{\partial \theta} \Delta p_\theta \quad (\beta = 1). \end{array} \right. \quad (1.16)$$

Now, this set of equations for $\Delta \vec{p}$ becomes surprisingly simple. It does not contain any source terms and is completely independent of boundaries, which can be conductors, resistive wall, dielectric, or even plasma. This result solely arises from the Maxwell equations plus the two approximations.

Table 1.1 Differential operators in the cylindrical coordinates. Here \vec{A} is a vector and ϕ is a scalar.

$$\begin{aligned} \vec{\nabla} \cdot \vec{A} &= \frac{1}{r} \frac{\partial}{\partial r} (rA_r) + \frac{1}{r} \frac{\partial A_\theta}{\partial \theta} + \frac{\partial A_s}{\partial s} \\ \vec{\nabla} \times \vec{A} &= \hat{r} \left(\frac{1}{r} \frac{\partial A_s}{\partial \theta} - \frac{\partial A_\theta}{\partial s} \right) + \hat{\theta} \left(\frac{\partial A_r}{\partial s} - \frac{\partial A_s}{\partial r} \right) + \hat{s} \left(\frac{1}{r} \frac{\partial (rA_\theta)}{\partial r} - \frac{1}{r} \frac{\partial A_r}{\partial \theta} \right) \\ \nabla^2 \phi &= \frac{1}{r} \frac{\partial}{\partial r} \left(r \frac{\partial \phi}{\partial r} \right) + \frac{1}{r^2} \frac{\partial^2 \phi}{\partial \theta^2} + \frac{\partial^2 \phi}{\partial s^2} \end{aligned}$$

There is no loss of generality to let $\Delta p_z \sim \cos m\theta$ with $m \geq 0$. Then, the three components of the impulse become

$$\Delta p_s = \Delta \tilde{p}_s \cos m\theta, \quad \Delta p_r = \Delta \tilde{p}_r \cos m\theta, \quad \text{and} \quad \Delta p_\theta = \Delta \tilde{p}_\theta \sin m\theta, \quad (1.17)$$

where $\Delta \tilde{p}_s$, $\Delta \tilde{p}_r$, and $\Delta \tilde{p}_\theta$ are θ -independent. The set of equations for $\Delta \tilde{p}$ becomes

$$\left\{ \begin{array}{l} \frac{\partial}{\partial r} (r \Delta \tilde{p}_\theta) = -m \Delta \tilde{p}_r, \\ \frac{\partial}{\partial z} \Delta \tilde{p}_r = \frac{\partial}{\partial r} \Delta \tilde{p}_s, \\ \frac{\partial}{\partial z} \Delta \tilde{p}_\theta = -\frac{m}{r} \Delta \tilde{p}_s, \\ \frac{\partial}{\partial r} (r \Delta \tilde{p}_r) = -m \Delta \tilde{p}_\theta \quad (\beta = 1). \end{array} \right. \quad (1.18)$$

From the first and last equations, we must have, for $m = 0$,

$$\Delta \tilde{p}_\theta = 0 \quad \text{and} \quad \Delta \tilde{p}_r = 0, \quad (1.19)$$

otherwise they will be proportional to r^{-1} which is singular at $r = 0$. From the same two equations, we get, for $m \neq 0$,

$$\frac{\partial}{\partial r} \left[r \frac{\partial}{\partial r} (r \Delta \tilde{p}_r) \right] = m^2 \Delta \tilde{p}_r, \quad (1.20)$$

and therefore

$$\Delta p_r(r, \theta, z) \sim r^{m-1} \cos m\theta. \quad (1.21)$$

Now the whole solution can be written as, for all $m \geq 0$,

$$\left\{ \begin{array}{l} v \Delta \tilde{p}_\perp = -q \mathcal{Q}_m W_m(z) m r^{m-1} (\hat{r} \cos m\theta - \hat{\theta} \sin m\theta), \\ v \Delta p_s = -q \mathcal{Q}_m W'_m(z) r^m \cos m\theta. \end{array} \right. \quad (1.22)$$

In above, $W_m(z)$ is called the *transverse wake function of azimuthal m* and $W'_m(z)$ the *longitudinal wake function of azimuthal m*. The latter is the derivative of the former. They are related because of the Panofsky–Wenzel theorem. The wake functions are functions of one variable z only, and are the only remaining unknowns. They are the only quantities that are dependent on the boundary conditions, and must be solved independently. Recall that the complicated Maxwell–Vlasov equation that involves \vec{E} , \vec{B} , and sources has been reduced drastically to solving just for $W_m(z)$.

More comments about Eq. (1.22) are in order. The original solution in the top line of Eq. (1.22) was for $m \neq 0$ only. However, we can always define a $W_0(z)$ which is the anti-derivative of $W'_0(z)$ so that the solution holds for all m . Although $W_0(z)$ has no physical meaning, yet it will be helpful in discussions below. In Eq. (1.22), q is the charge of the test particle and Q_m is the electric m th multipole of the source particle. For a source particle of charge e at an offset a from the axis of the cylindrical beam pipe, $Q_m = ea^m$. Thus, W'_m has the dimension of force per charge square per length^($2m-1$) or Volts/Coulomb/m ^{$2m$} , while W_m has the dimension of force per charge square per length ^{$2m$} or Volts/Coulomb/m ^{$2m-1$} . The negative signs on the right sides arise just from a convention. For example, we want the longitudinal wake $W'_m(z)$ to be positive when the impulse acting on the test particle is decelerating.

Sometimes the wake functions are listed in the CGS units in literature, and W_m has the CGS dimension of length ^{$-2m$} . The conversion consists of simply multiplying the wake functions in the CGS units by the factor $Z_0c/(4\pi) = 0.898755 \times 10^{10}$. Thus a dipole transverse wake of $W_1 = 1 \times 10^5 \text{ m}^{-2}$ corresponds to $W_1 = 0.898755 \times 10^{15} \text{ V}/(\text{Coulomb}\cdot\text{m})$.

Recall that we have been looking at the wake force on a particle traveling at $s = z + vt$ behind a source particle traveling at $s = vt$. Thus $z < 0$. When $v \rightarrow c$, causality has to be imposed that $W_m(z) = 0$ when $z > 0$. For our discussions below, we will continue to use v instead of c in most places, because we would like to derive stability conditions and growth rates also for machines that are not ultra-relativistic. However, strict causality will be imposed as if the velocity is c . So far, the derivation has been in the time domain. All variables, like the charge distribution ρ , the electromagnetic fields \vec{E} and \vec{B} , the wake force \vec{F} , the impulse $\Delta\vec{p}$, etc, are real quantities. Thus the wake functions $W_m(z)$'s are also real functions.

Immediately behind a source particle, the test particle should receive a retarding force, otherwise a particle will continue to gain energy as it is traveling down the vacuum chamber in direct violation of the conservation of energy. This implies that $W'_m(z) > 0$ when $|z|$ is small, recalling that the $W'_m(z)$ is defined in Eq. (1.22) with a negative sign on the right side. This is illustrated in Fig. 1.3. It will be proved later in Chapter 7 that a particle sees half of its own wake. For the transverse wake $W_m(z)$, it starts out from zero[†] and goes negative as $|z|$ increases, as required by the Panofsky-Wenzel theorem. Thus, when the source particle is deflected, a transverse wake force is created in the direction that it will deflect particles immediately following in the *same* direction of the deflection of the source. Again, special attention should be paid to the negative

[†]Although it cannot be proved that $W_m(0) = 0$, however, most wakes do have this property.

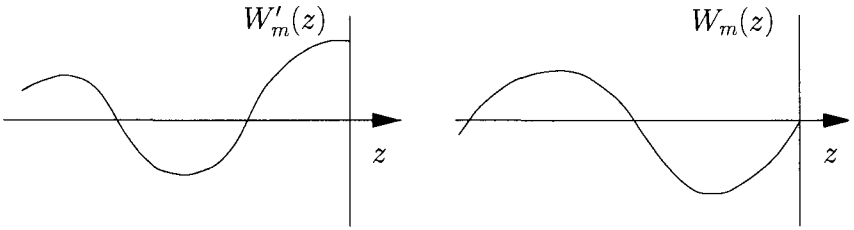


Fig. 1.3 The longitudinal wake $W'_m(z)$ vanishes when $z > 0$ and is positive definite when $|z|$ is small. The transverse wake $W_m(z)$ starts out from zero and goes negative as z decreases when $|z|$ is small.

sign on the right side of the definition of $W_m(z)$ in Eq. (1.22). The transverse wake W_m vanishes at $z = 0$ implies that a particle will not see its own transverse wake at all. This leads to the important conclusion that a shorter bunch will be preferred if the transverse wake dominates, and a longer bunch will be preferred if the longitudinal wake dominates.

When $m = 0$ or the monopole, we have $\Delta p_{\perp} = 0$ while Δp_s is independent of (r, θ) and depends only on z . Thus, particles in a thin transverse slice of the beam will see the same impulse in the s -direction according to the dependence of W'_0 on z , as shown in Fig. 1.4. This impulse can lead to self-bunching or microwave instability.

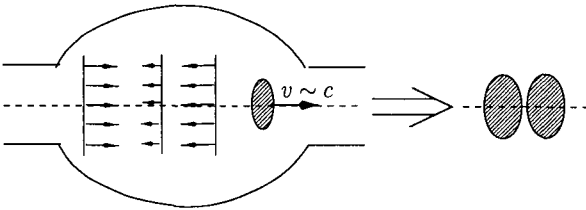


Fig. 1.4 All particles in a vertical slice of the beam see exactly the same monopole wake impulse ($m = 0$) from the source according to the slice position z behind the source. This longitudinal variation of impulse effect on the slices can lead to longitudinal microwave instability.

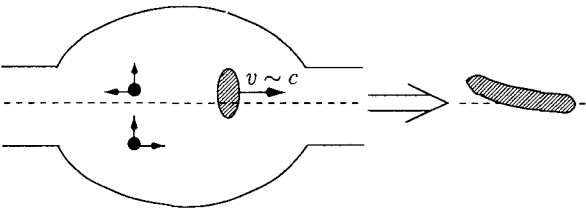


Fig. 1.5 Transverse kicks for all the particles in a vertical slice from the dipole wake impulse have the same magnitude; however, the longitudinal kicks point to forward or backward direction depending on whether the particles are above or below the axis of symmetry.

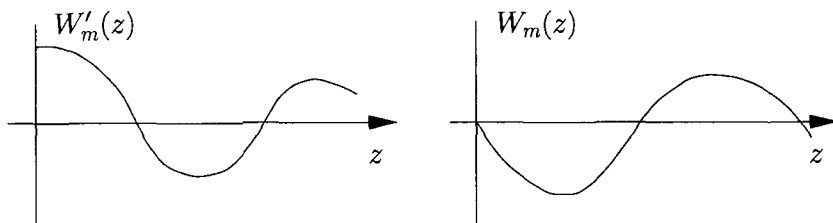


Fig. 1.6 This is a different convention that the wake functions $W_m(z)$ vanish when $z < 0$. Since the physics is the same, the wake functions are the same as in Fig. 1.3 and just the direction of z has been changed. In this convention, the interpretation $W'_m(z) \equiv -\frac{d}{dz}W_m(z)$ is required.

For $m = 1$, we have from Eq. (1.22) that Δp_{\perp} is independent of (r, θ) but depends on z only. All particles in a vertical slice of the beam suffer exactly the same vertical kick from the dipole wake impulse ($m = 1$) which depends only on how far the slice is behind the dipole source, and will be kicked in the same transverse direction, as is shown in Fig. 1.5. Such an impulse can lead to the tilting of the tail of the bunch into a banana shape. Particle loss will occur when the tilted bunch hits the vacuum chamber. This is the cause of beam breakup. On the other hand, the dipole longitudinal impulse Δp_s ($m = 1$) is proportional to the offset of the test particle in the x -direction. Thus particles on opposite sides of the axis of the vacuum chamber will be driven longitudinally in the opposite directions.

For the sake of convenience, many authors do not like to work with a negative z for the particles that are following. There is another convention that $W_m(z) = 0$ when $z < 0$. This does not change the physics and the direction of the wake forces will not be changed. Thus, instead of Fig. 1.3, we have Fig. 1.6 instead. A price has to be paid for this convention. We must interpret the connection between the longitudinal and transverse wakes as

$$W'_m(z) \equiv -\frac{d}{dz}W_m(z). \quad (1.23)$$

This convention will be used for the rest of the book.[§] Fortunately, we will not be using Eq. (1.23) much below, because most longitudinal instabilities are driven dominantly by the monopole longitudinal wake W'_0 and most transverse instabilities are driven dominantly by the dipole transverse wake W_1 . We will have a brief investigation of the quadrupole wake function in Chapter 14.

[§]The readers should be aware of yet another convention in the literature that $W_m(z)$ and $W'_m(z)$ are defined in Eq. (1.22) *without* the negative signs on the right sides. The wake functions, however, will have just the opposite signs of what are depicted in Fig. 1.6.

1.2 Coupling Impedances

Beam particles form a current, of which the component with frequency $\omega/(2\pi)$ is[†] $I(s, t) = \hat{I}e^{-i\omega(t-s/v)}$, where \hat{I} may be complex. Let us concentrate on a very short section Δs_1 of the cylindrical vacuum chamber at s_1 and assume that the vacuum chamber does not generate any wake outside this section. A test particle at location s_1 at time t will be affected by the wake left behind by the preceding charge element $I(s_1, t-z/v)dz/v$ that passes the point s_1 at time $t-z/v$ earlier. The *accelerating* voltage seen (or energy gained per unit test charge) is

$$V(s_1, t) = - \int_{-\infty}^{\infty} \hat{I} e^{-i\omega[t-(s_1+z)/v]} [W'_0(z)]_1 \frac{dz}{v} = -I(s_1, t) \int_{-\infty}^{\infty} e^{i\omega z/v} [W'_0(z)]_1 \frac{dz}{v}, \quad (1.24)$$

where $[W'_0(z)]_1$ is wake function for the small section of the vacuum chamber at s_1 . If we write the potential across the section at s_1 as $V(s_1, t) = \hat{V}_1 e^{-i\omega(t-s_1/v)}$, the above simplifies to

$$\hat{V}_1 = -\hat{I} \int_{-\infty}^{\infty} e^{i\omega z/v} [W'_0(z)]_1 \frac{dz}{v}. \quad (1.25)$$

Thus, we can identify the *longitudinal coupling impedance* of this small section of the vacuum chamber at s_1 as

$$[Z_0^{\parallel}(\omega)]_1 = \int_{-\infty}^{\infty} e^{i\omega z/v} [W'_0(z)]_1 \frac{dz}{v}, \quad (1.26)$$

where the lower limit has been extended to $-\infty$ because of the causal property of the wake function. This definition is the same as the ordinary impedance in a circuit. Notice that $q\hat{V}_1 = F^{\parallel}(s_1)\Delta s_1$, and the latter is just the integrated longitudinal wake force across the small section at s_1 . Unlike the integrated wake force (or the longitudinal impulse Δp_s), however, $V(s_1, t)$ in general complex. This is because we have been using a current wave as the source in the complex representation.

Next let us consider the adjacent section of the vacuum chamber at s_2 and assume the rest of the vacuum chamber does not generate any wake. We then obtain the potential $V(s_2, t) = \hat{V}_2 e^{-i\omega(t-s_2/v)}$ across this section as

$$\hat{V}_2 = -\hat{I} [Z_0^{\parallel}(\omega)]_2, \quad (1.27)$$

[†] We are going to use the physicist convention of frequency dependence $e^{-i\omega t}$, which leads to the results that the capacitive impedance is positive imaginary while the inductive impedance is negative imaginary. The opposite is true in the engineer convention of $e^{j\omega t}$.

where $[Z_0^{\parallel}(\omega)]_2$, given by Eq. (1.26) with the subscript 1 replaced by 2, is the coupling impedance for this small section at s_2 . When all these small sections are added up, $\sum_i [W'_0(z)]_i = W'_0(z)$, which is the wake function of the whole vacuum chamber, and $Z_0^{\parallel}(\omega) = \sum_i [Z_0^{\parallel}(\omega)]_i$, or

$$Z_0^{\parallel}(\omega) = \int_{-\infty}^{\infty} e^{i\omega z/v} W'_0(z) \frac{dz}{v} \quad (1.28)$$

becomes the longitudinal coupling impedance of the whole vacuum chamber.

We have here much more than in a circuit because, unlike a current in a resistive wire, the beam current possesses transverse distribution thus leading to higher multipoles, for example, when the current is displaced horizontally by a from the axis of symmetry of the cylindrical vacuum chamber. Let us concentrate now on the m th multipole of the current

$$\mathcal{P}_m(s, t) = I(s, t) a^m = \hat{\mathcal{P}}_m e^{-i\omega(t-s/v)}, \quad (1.29)$$

where $\hat{\mathcal{P}}_m = \hat{I} a^m$. Consider a test particle of charge q at $x = a$ in the beam traveling with velocity v in the s -direction. Its charge density is given by

$$\begin{aligned} \rho(r, \theta, s; t) &= \frac{q}{a} \delta(r - a) \delta(\theta) \delta(s - vt) \\ &= \sum_{m=0}^{\infty} \frac{\mathcal{Q}_m}{(1 + \delta_{m0}) \pi a^{m+1}} \delta(r - a) \cos m\theta \int_{-\infty}^{\infty} \frac{d\omega}{2\pi v} e^{-i\omega(t-s/v)}, \end{aligned} \quad (1.30)$$

where $\mathcal{Q}_m = qa^m$ denotes the electric m th multipole of the test particle. Again assume that the vacuum chamber does not generate any wake fields except for a short section of length Δs_i at s_i . At location s_i and time t , the test particle will see the wake left behind by the preceding charge m th-multipole element in the beam, $\mathcal{P}(s_i, t - z/v) dz/v$, that passes the location s_i at time $t - z/v$. The total accelerating voltage seen by the test particle across this small section is, according to the longitudinal wake force in Eq. (1.22),

$$V(s_i, t) = - \int_{-\infty}^{\infty} \frac{dz}{v} \mathcal{P}_m(s_i, t - z/v) [W'_m(z)]_i \int r dr d\theta r^m \cos m\theta \frac{\delta(r - a) \delta(\theta)}{a}, \quad (1.31)$$

where $[W'_m(z)]_i$ is the m th-multipole wake function for this small section of the vacuum chamber at s_i , and the charge density of the test particle has been inserted. For consistency, it is easy to check that Eq. (1.31) reduces to Eq. (1.24) when $m = 0$. Obviously, only the m th multipole of the charge density contributes

and we obtain after integrating over r and θ ,

$$\hat{V}_1 = -\frac{\hat{\mathcal{P}}_m \mathcal{Q}_m}{q} \int_{-\infty}^{\infty} \frac{dz}{v} e^{-i\omega z/v} [W'_m(z)]_i. \quad (1.32)$$

Summing up the contribution of all small sections of the vacuum chamber, we obtain the total potential difference, $\hat{V} = \sum_i \hat{V}_i$, across the whole vacuum chamber in terms of the total m th-multipole wake function $W'_m(z) = \sum_i [W'_m(z)]_i$,

$$\hat{V} = -\frac{\hat{\mathcal{P}}_m \mathcal{Q}_m}{q} \int_{-\infty}^{\infty} \frac{dz}{v} e^{-i\omega z/v} W'_m(z). \quad (1.33)$$

Following Eq. (1.28), we identify

$$Z_m^{\parallel}(\omega) = \int_{-\infty}^{\infty} e^{i\omega z/v} W'_m(z) \frac{dz}{v} \quad (1.34)$$

as the longitudinal coupling impedance of the vacuum chamber in the m th multipole. Physically, this is equal to the decelerating voltage seen by one unit of test charge multipole \mathcal{Q}_m in a beam of unit current m th multipole \mathcal{P}_m . Correspondingly, the *transverse coupling impedance of the m th multipole* is defined as

$$Z_m^{\perp}(\omega) = \frac{i}{\beta} \int_{-\infty}^{\infty} e^{i\omega z/v} W_m(z) \frac{dz}{v}. \quad (1.35)$$

Recalling that $W'_m(z) = -dW_m(z)/dz$, we have therefore $Z_m^{\parallel}(\omega) = \omega Z_m^{\perp}(\omega)/c$. Since $\text{Re } Z_1^{\perp}(\omega) > 0$ when $\omega > 0$ is required by the Panofsky–Wenzel theorem [see Eq. (1.49)], the oscillatory motion of the multipole \mathcal{P}_m is seeing a transverse wake force F_m^{\perp} that opposes its motion. Thus F_m^{\perp} must lag the dipole by $\pi/2$ in order to dissipate its energy, and hence the factor $-i$ in Eq. (1.43).[‡] The Lorentz factor $\beta = v/c$ is inserted to cancel the velocity in the Lorentz force.[§]

We learn from the above derivation that the longitudinal impedance in the m th multipole corresponds essentially to the energy lost to the m th multipole current when the m th-multipole wake force is encountered. In fact, we can write

$$q\hat{V} = \sum_i [F_m^{\parallel}]_i \Delta s_i = \int_0^L F_m^{\parallel}(s) ds, \quad (1.36)$$

where $[F_m^{\parallel}]_i$ is the m th-multipole wake force experienced at the small section at s_i with the factor $e^{-i\omega(t-s_i/v)}$ removed. Since the m th multipole wake force has

[‡]In the $e^{-i\omega t}$ convention, phase advances clockwise as time progresses. Thus a phase lead/lag implies $e^{-i\psi}$ with $\psi \geq 0$.

[§]Some authors define the transverse impedance without the factor β in the denominator.

a transverse distribution proportional to $r^m \cos m\theta$, its evaluation in Eq. (1.36) should be at $r = a$ and $\theta = 0$, the offset position of the original beam current or the test particle. Instead, Eq. (1.36) can be rewritten more conveniently as

$$q\hat{V} = \frac{1}{\bar{I}} \int_0^L F_m^{\parallel}(s, r, \theta) J_m^* dV, \quad (1.37)$$

where ¶

$$J_m(r, \theta, s; t) = \frac{\hat{P}_m}{(1 + \delta_{m0})\pi a^{m+1}} \delta(r - a) \cos m\theta e^{-i\omega(t-s/v)} \quad (1.38)$$

is the m th-multipole current density in the same longitudinal direction of the longitudinal wake force, and the volume integral is performed with $dV = r dr d\theta ds$ ranging over the cross section and the length of the vacuum chamber.

Following Eq. (1.31), the coupling impedance $Z_m^{\parallel}(\omega)$ can be expressed as in terms of the wake force $F^{\parallel}(s, r, \theta)$ experienced by a test particle along the vacuum chamber,

$$Z_m^{\parallel}(\omega) = -\frac{1}{q\hat{P}_m^2} \int_0^L F_m^{\parallel} J_m^* dV, \quad (1.39)$$

in a form which can be used more easily in computation. In above, and wake force F_m^{\parallel} is allowed to include the exponential factor $e^{-i\omega(t-s/v)}$ and this factor is cancelled when it is multiplied by the complex conjugate of J_m . The transverse impedance in the m th multipole is then given by

$$Z_m^{\perp}(\omega) = -\frac{c}{\omega q\hat{P}_m^2} \int_0^L F_m^{\parallel} J_m^* dV. \quad (1.40)$$

In Eqs. (1.39) and (1.40), q is the charge of a test particle, so that $F_m^{\parallel}(r, \theta, s; t)/q = E^{\parallel}(r, \theta, s; t)$ is the longitudinal electric field experienced by the beam particle. It is important to point out that in Eq. (1.39) or Eq. (1.40), the integration over ds covers just the length L of the beam pipe and in the case of a circular ring, L is usually taken as the ring circumference C . Thus, the integral represents an average of the wake force around the circumference of the ring. On the other hand, in Eq. (1.28), (1.34) or (1.35), the longitudinal integration is over z , the distance behind the source particle, and the upper limit has to be taken to $+\infty$ unless the wake is short.

¶Here we consider J_m to have the dimension of current density. If it is considered as a frequency Fourier component instead, so that the total current density is $\int d\omega J_m$, it carries the dimension of current density multiplied by time, and Eqs. (1.37), (1.39), and (1.40) will require suitable adjustment.

The transverse impedance can also be expressed in terms of the transverse wake force, because there Panofsky–Wenzel theorem relates the longitudinal and transverse wake forces. Let us concentrate on the dipole contribution ($m = 1$). For an infinitesimal offset ($a \rightarrow 0$), the dipole current density can be written as^{||}

$$J_1(r, \theta, s; t) = \frac{\mathcal{P}_1}{2a} [\delta(x - a) - \delta(x + a)] e^{-i\omega(t-s/v)}. \quad (1.41)$$

Then the dipole impedance in the horizontal direction is

$$\begin{aligned} Z_1^x(\omega) &= -\frac{c}{\omega q \mathcal{P}_1} \int_0^L F_1^{\parallel} \frac{[\delta(x - a) - \delta(x + a)]}{2a} \delta(y) e^{i\omega(t-s/v)} dV \\ &= -\frac{c}{\omega q \mathcal{P}_1} \int_0^L \frac{\partial F_1^{\parallel}}{\partial x} e^{i\omega(t-s/v)} dz, \end{aligned} \quad (1.42)$$

where F_1^{\parallel} , evaluated at $x = a$ and $y = 0$, is the longitudinal dipole wake force in the s -direction including the factor $e^{-i\omega(t-s/v)}$. Finally, employing Panofsky–Wenzel theorem in the form of Eq. (1.12), we obtain

$$Z_1^{\perp}(\omega) = -\frac{i}{\beta q \mathcal{P}_1} \int_0^L F_{1x} e^{i\omega(t-s/v)} dz, \quad (1.43)$$

where F_{1x} is the horizontal wake force. Thus the transverse dipole impedance is just the average integrated transverse wake force generated by a unit dipole current experienced by a particle of unit charge.

The transverse dipole impedance can also be derived directly from the transverse dipole wake force F_1^{\perp} without going into the longitudinal wake force F_1^{\parallel} . When the current is displaced transversely by a from the axis of symmetry of the beam pipe, the *deflecting* transverse force acting on a current particle is obtained by summing the charge element $I(s, t - z/v) dz/v$ passing s at time $t - z/v$,

$$\begin{aligned} \langle F_1^{\perp}(s, t) \rangle &= -\frac{qa}{L} \int_{-\infty}^{\infty} \hat{I} e^{-i\omega[t-(s+z)/v]} W_1(z) \frac{dz}{v} \\ &= -\frac{qa}{L} I(s, t) \int_{-\infty}^{\infty} e^{i\omega z/v} W_1(z) \frac{dz}{v}, \end{aligned} \quad (1.44)$$

where $\langle F_1^{\perp}(s, t) \rangle$ is the transverse force of frequency ω in the direction of the displacement averaged over a length L covering the discontinuity of the vacuum chamber, and is therefore equal to $v\Delta p_{\perp}/L$, with Δp_{\perp} being the transverse impulse studied in the previous section. With the definition of the dipole transverse

^{||}Essentially, as $a \rightarrow 0$, we have $\frac{1}{\pi a^2} \delta(r - a) \cos \theta = \frac{1}{2a} [\delta(x - a) - \delta(x + a)] \delta(y)$. The dipole moment results when multiplied by qa and integrated over the cross-sectional area.

coupling impedance of the vacuum chamber given by Eq. (1.35), we get back Eq. (1.43).

We learn that the coupling impedances are the Fourier transforms of the corresponding wake functions. The wake functions can be written in terms of the impedances as inverse Fourier transforms:

$$W_m(z) = -\frac{i\beta}{2\pi} \int_{-\infty}^{\infty} Z_m^\perp(\omega) e^{-i\omega z/v} d\omega, \quad (1.45)$$

$$W'_m(z) = \frac{1}{2\pi} \int_{-\infty}^{\infty} Z_m^\parallel(\omega) e^{-i\omega z/v} d\omega, \quad (1.46)$$

where the path of integration in both cases is above all the singularities of the impedances so as to guarantee causality.

Note that the longitudinal impedance is mostly the monopole ($m = 0$) impedance and the transverse impedance is mostly the dipole ($m = 1$) impedance, if the beam pipe cross section is close to circular and the particle path is close to the pipe axis. They have the dimensions of Ohms and Ohms/length, respectively. The impedances have the following properties:**

1. $Z_m^\parallel(-\omega) = [Z_m^\parallel(\omega)]^*$ and $Z_m^\perp(-\omega) = -[Z_m^\perp(\omega)]^*$. (1.47)

2. $Z_m^\parallel(\omega)$ and $Z_m^\perp(\omega)$ are analytic with poles only in the lower half ω -plane. (1.48)

3. $Z_m^\parallel(\omega) = \frac{\omega}{c} Z_m^\perp(\omega)$, for cylindrical geometry and each azimuthal harmonic including $m = 0$. (1.49)

4. $\text{Re } Z_m^\parallel(\omega) \geq 0$ and $\text{Re } Z_m^\perp(\omega) \geq 0$ when $\omega > 0$, if the beam pipe has the same entrance cross section and exit cross section. (1.50)

5. $\int_0^\infty d\omega \text{Im } Z_m^\perp(\omega) = 0$, and $\int_0^\infty d\omega \frac{\text{Im } Z_m^\parallel(\omega)}{\omega} = 0$. (1.51)

The first follows because the wake functions are real, the second from the causality of the wake functions, and the third from the Panofsky–Wenzel theorem [2] between transverse and longitudinal electromagnetic forces. $\text{Re } Z_m^\parallel(\omega) \geq 0$ is the result of the fact that the total energy of a particle or a bunch cannot be increased after passing through a section of the vacuum chamber where there is no accelerating external forces, while $\text{Re } Z_m^\perp(\omega) \geq 0$ when $\omega > 0$ follows from

**In Property 2, if we adopt the $e^{j\omega t}$ convention instead, all the singularities will be in the upper half plane. In Property 3, Z_0^\perp may not have any physical meaning. But it is a well-defined quantity mathematically.

the Panofsky–Wenzel theorem. The fifth property follows from the assumption that $W_m(0) = 0$.

For a pure resistance R , the longitudinal wake is $W'_0(z) = R\delta(z/v)$. At low frequencies, the wall of the beam pipe is inductive. This wake function is $W'_0(z) = \mathcal{L}\delta'(z/v)$, where \mathcal{L} is the inductance.

For a nonrelativistic beam of radius a inside a circular beam pipe of radius b , the longitudinal space-charge impedance for $m = 0$ is^{††}

$$Z_0^{\parallel}(\omega) = i\frac{\omega}{\omega_0} \frac{Z_0}{2\gamma^2\beta} \left(1 + 2\ln\frac{b}{a}\right), \quad (1.52)$$

where $Z_0 = \sqrt{\mu_0/\epsilon_0} \approx 377 \Omega$ is the impedance of free space, μ_0 and ϵ_0 are, respectively, the magnetic permeability and electric permittivity of free space, $\omega_0/(2\pi)$ is the revolution frequency of the beam particle with Lorentz factors γ and β . Although this impedance is capacitive, however, it appears in the form of a negative inductance. The corresponding wake function is

$$W'_0(z) = -\delta'(z/v) \frac{1}{\omega_0} \frac{Z_0}{2\gamma^2\beta} \left(1 + 2\ln\frac{b}{a}\right). \quad (1.53)$$

The $m = 1$ transverse space-charge impedance for a length L of the circular beam pipe is

$$Z_1^{\perp}(\omega) = i\frac{Z_0L}{2\pi\gamma^2\beta^2} \left[\frac{1}{a^2} - \frac{1}{b^2}\right], \quad (1.54)$$

and the corresponding transverse wake function is

$$W_1(z) = \frac{Z_0cL}{2\pi\gamma^2} \left[\frac{1}{a^2} - \frac{1}{b^2}\right] \delta(z). \quad (1.55)$$

The space-charge impedances will be derived in Chapter 2.

An important impedance is that of a resonant cavity. Near the resonant frequency $\omega_r/(2\pi)$, the m th multipole longitudinal impedances can be approximated by a *RLC*-parallel circuit:

$$Z_m^{\parallel}(\omega) = \frac{R_{ms}}{1 + iQ\left(\frac{\omega_r}{\omega} - \frac{\omega}{\omega_r}\right)}, \quad (1.56)$$

where the resonant angular frequency is $\omega_r = (\mathcal{L}_m C_m)^{-1/2}$ and quality factor is $Q = R_{ms}\sqrt{C_m/\mathcal{L}_m}$. Here, for the m th multipole, the shunt impedance R_{ms}

^{††}This expression will be derived in Sec. 2.4. Here, the space-charge force is seen by beam particles at the beam axis. If the force is averaged over the cross section of the beam with a uniform transverse cross section, the first term in the brackets becomes $\frac{1}{2}$ instead of 1.

is in Ohms/m^{2m}, the inductance \mathcal{L}_m in henry/m^{2m}, and the capacitance C_m in farad-m^{2m}. The transverse impedance can now be obtained from the Panofsky-Wenzel theorem of Eq. (1.49):

$$Z_m^\perp(\omega) = \frac{c}{\omega} \frac{R_{ms}}{1 + iQ \left(\frac{\omega_r}{\omega} - \frac{\omega}{\omega_r} \right)}. \quad (1.57)$$

Another example is the longitudinal impedance for a length L of the resistive beam pipe:

$$Z_0^\parallel(\omega) = [1 - i \operatorname{sgn}(\omega)] \frac{L}{2\pi b \sigma_c \delta_{\text{skin}}}, \quad (1.58)$$

where b is the radius of the cylindrical beam pipe, σ_c is the conductivity of the pipe wall,

$$\delta_{\text{skin}} = \sqrt{\frac{2c}{Z_0 \mu_r \sigma_c |\omega|}} \quad (1.59)$$

is the skin-depth at frequency $\omega/(2\pi)$, and μ_r is the relative magnetic permeability of the pipe wall. The transverse impedance is

$$Z_1^\perp(\omega) = [1 - i \operatorname{sgn}(\omega)] \frac{Lc}{\pi \omega b^3 \sigma_c \delta_{\text{skin}}}, \quad (1.60)$$

and is related to the longitudinal impedance by

$$Z_1^\perp(\omega) = \frac{2c}{b^2 \omega} Z_0^\parallel(\omega). \quad (1.61)$$

The above relation has been used very often to estimate the transverse impedance from the longitudinal. However, we should be aware that this relation holds only for resistive impedances of a cylindrical beam pipe. The monopole longitudinal impedance and the dipole transverse impedance belong to different azimuthals; therefore they should not be related. An example that violates Eq. (1.61) is the longitudinal and transverse space-charge impedances stated in Eqs. (1.52) and (1.54).

The expression of the transverse resistive-wall impedance as given by Eq. (1.60) is not quite correct because it indicates a divergency as $\omega^{-1/2}$ at low frequencies. Actually, $\mathcal{I}m Z_1^\perp$ approaches a constant as $\omega \rightarrow 0$ while $\mathcal{R}e Z_1^\perp$ bends around and approaches zero. These behaviors have important bearing on transverse coupled-bunch instabilities, which we will address in Chapter 10.

More expressions for wakes and impedances resulting from various types of discontinuity in the vacuum chamber are listed in the Appendix. [4] Readers that have interest in deriving these and other expressions of impedances should

consult the books or articles written by Chao, Gluckstern, as well as Zotter and Kheifets. [3, 15, 16]

1.3 Parasitic Loss

A beam particle inside a vacuum chamber loses energy in three ways: through synchrotron radiation when its path is bent by the magnetic dipole fields of the accelerator lattice, through interaction with the wake fields left by preceding beam particles, and through interaction with the residual gas molecules. In this section, we are going to concentrate on the energy loss through wake fields. This loss is also known as parasitic loss.

1.3.1 Coherent Loss

Consider a bunch having linear distribution $\lambda(\tau)$ that is normalized to unity,

$$\int_{-\infty}^{\infty} \lambda(\tau) d\tau = 1. \quad (1.62)$$

A beam particle is referenced by τ , its time of arrival at a designated point in the accelerator ring ahead of the synchronous particle (see Sec. 2.1.1). The bunch is considered stationary and its time dependency has therefore been omitted in this consideration. The energy *gained* experienced by this particle in a revolution turn is, according to Eq. (1.22),

$$\Delta\mathcal{E}(\tau) = -e^2 N_b \int_{-\infty}^{\tau} d\tau' W'_0(\tau - \tau') \lambda(\tau'), \quad (1.63)$$

where N_b is the total number of beam particles in the bunch. In the frequency space, with*

$$\tilde{\lambda}(\omega) = \frac{1}{2\pi} \int_{-\infty}^{\infty} d\tau \lambda(\tau) e^{-i\omega\tau}, \quad (1.64)$$

the energy gained by the beam particle can be represented by

$$\Delta\mathcal{E}(\tau) = -e^2 N_b \int_{-\infty}^{\infty} d\omega \tilde{\lambda}(\omega) Z_0^{\parallel}(\omega) e^{-i\omega\tau}, \quad (1.65)$$

where Eq. (1.46) has been used. We see that particles at different arrival time τ gain energy differently. When averaged over all the particles in the bunch, the

*The reader should be aware that the definition of the Fourier transform, with or without the factor $(2\pi)^{-1}$ in front of the integral, will affect the expressions for energy gain below.

average energy gain per particle per turn is given by

$$\overline{\Delta\mathcal{E}} = \int_{-\infty}^{\infty} d\tau \lambda(\tau) \mathcal{E}(\tau) = -2\pi e^2 N_b \int_{-\infty}^{\infty} d\omega |\tilde{\lambda}(\omega)|^2 Z_0^{\parallel}(\omega). \quad (1.66)$$

Notice that

$$\begin{aligned} |\tilde{\lambda}(\omega)|^2 &= \frac{1}{(2\pi)^2} \int_{-\infty}^{\infty} d\tau \int_{-\infty}^{\infty} d\tau' \lambda(\tau) \lambda(\tau') e^{-i\omega(\tau-\tau')} \\ &= \frac{1}{(2\pi)^2} \int_{-\infty}^{\infty} d\tau \int_{-\infty}^{\infty} d\tau' \lambda(\tau) \lambda(\tau') \cos[\omega(\tau-\tau')]. \end{aligned} \quad (1.67)$$

Since $|\tilde{\lambda}(\omega)|^2$ is real and is symmetric in ω , only $\Re Z_0^{\parallel}$ contributes in Eq. (1.66). For a bunch in a circular beam pipe of radius b and Gaussian distributed linearly with rms length σ_τ , the parasitic energy gained per revolution turn can be computed straightforwardly using the longitudinal resistive-wall impedance given in Eq. (1.58), and the result is

$$\Delta\mathcal{E}_{\text{bunch}} = -\frac{e^2 N_b^2 R \Gamma(\frac{3}{4})}{2\pi b \sigma_\tau^{3/2}} \left(\frac{Z_0 \mu_r}{2\sigma_c c} \right)^{1/2}, \quad (1.68)$$

where μ_r and σ_c are, respectively, the relative magnetic permeability and electric conductivity of the beam pipe, R is the mean radius of the accelerator ring, and $\Gamma(\frac{3}{4}) = 1.22542$ is the Gamma function.

The Fourier transform of the linear density has not been performed correctly. [5] In the absence of focusing by the rf system, the linear density $\lambda(\tau)$ is periodic in τ with period $T_0 = 2\pi/\omega_0$. The Fourier transform is therefore discrete. The correct Fourier expansion should be

$$\lambda(\tau) = \frac{2\pi}{T_0} \sum_{n=-\infty}^{\infty} \tilde{\lambda}_n e^{in\omega_0\tau}. \quad (1.69)$$

Instead of Eq. (1.64), the Fourier transform is

$$\tilde{\lambda}_n = \frac{1}{2\pi} \int_{-T_0/2}^{T_0/2} d\tau \lambda(\tau) e^{-in\omega_0\tau}, \quad (1.70)$$

with the energy gain per turn

$$\Delta\mathcal{E}(\tau) = -e^2 N_b \omega_0 \sum_{n=-\infty}^{\infty}{}' \lambda_n Z_0^{\parallel}(n\omega_0) e^{in\omega_0\tau}, \quad (1.71)$$

where the primed summation runs over all nonzero integer n and the exclusion of $n = 0$ will be explained below. An unconventional constant has been placed

in front of the summation in the harmonic expansion of Eq. (1.69) so that the discrete Fourier transform $\tilde{\lambda}_n$ of Eq. (1.70) has similar definition as the non-periodic transform $\tilde{\lambda}(\omega)$ of Eq. (1.64). This also results in the average energy gain per particle per turn

$$\overline{\Delta\mathcal{E}} = -2\pi e^2 N_b \omega_0 \sum_{n=-\infty}^{\infty} |\tilde{\lambda}_n|^2 \operatorname{Re} Z_0^{\parallel}(n\omega_0), \quad (1.72)$$

which is very similar to the corresponding one, Eq. (1.66), in the non-periodic expansion.

When the bunch is short, there is not much difference between Eqs. (1.66) and (1.72), because the spectrum of the bunch extends to very high frequencies and therefore many harmonics. However, for very long bunches, the difference can become very big. This is reflected by the fact that the Fourier transform of the linear density in Eq. (1.64) is clearly invalid mathematically when the bunch nearly fills up the ring longitudinally. As an example, a long bunch of length τ_0 in the Fermilab Recycler Ring confined between two barrier waves usually has sharp edges longitudinally and may occupy over 80% of the ring. In this case, only very few low harmonics will contribute. If the linear density is represented by

$$\lambda(\tau) = \begin{cases} \frac{1}{\tau_0} & |\tau| < \frac{\tau_0}{2}, \\ 0 & \text{otherwise,} \end{cases} \quad (1.73)$$

the power spectrum is, for any integer n from $-\infty$ to $+\infty$,

$$|\tilde{\lambda}_n|^2 = \frac{1}{(2\pi)^2} \left(\frac{\sin n\omega_0\tau_0/2}{n\omega_0\tau_0/2} \right)^2. \quad (1.74)$$

Let us examine the lower harmonics. First, the zero harmonic (or dc component) does not contribute to the parasitic loss even if $\operatorname{Re} Z_0^{\parallel} \neq 0$. The $n = 0$ component of a beam is static because there is no time dependency.[†] As a result, electric field and magnetic field in the Maxwell equations are separated. There is no more Faraday's law. Thus, the static magnetic field of the beam's dc component does not induce any electric field on the surface or inside the wall of the beam pipe. In other words, there is no image current corresponding to the dc component of the beam, resulting in zero energy loss. For the dc component, what is present in the wall of the beam pipe is just static (nonmoving) image charges. For the

[†]One may argue that the dc component is also time varying because the revolution frequency of the beam is changing when the rf voltage is turned off. However, this change is extremely slow, for example, only 0.032 Hz in an hour in the Fermilab Recycler Ring.

other low harmonics, the argument of sine,

$$\frac{n\omega_0\tau_0}{2} = n\pi\frac{\tau_0}{T_0} \quad (1.75)$$

is close to $n\pi$ if the bunch length is nearly as long as the circumference of the ring. Thus, the energy loss per turn will be very small. For example, if $\tau_0/T_0 = 0.82$, $|\tilde{\lambda}_n|^2 = 0.00110, 0.00078, 0.00042, 0.00014, \dots$, respectively, for $n = \pm 1, \pm 2, \pm 3, \pm 4, \dots$, indicating that only a few low harmonics are important. On the other hand, if the non-periodic expression of Eq. (1.66) is used instead, the large $\sin x/x$ peak will have been partially included in an incorrect way, even with a $\text{Re } Z_0^{\parallel}$ that goes to zero at zero frequency. Notice that, as the bunch length continues to increase to fill up the whole ring, the power spectrum $|\tilde{\lambda}_n|$ falls to zero except for $n = 0$, implying that the parasitic loss approaches zero. On the other hand, in the non-periodic expansion, the parasitic loss given by Eq. (1.65) will never go to zero.

1.3.2 Incoherent Loss

The energy loss expressions derived above are for *coherent* energy loss, implying that only the loss due to the coherent spectrum has been taken into account. This can be understood by realizing that we have been referring to the power spectrum of a bunch but not the spectrum of the individual particles. For this reason, the total energy loss by the bunch is proportional to N_b^2 and the per particle energy loss is proportional to N_b .

For a true coasting beam, the arrival time of a beam particle at a designated point of the accelerator ring is random. The image current will be the *incoherent sum* of the image current coming from each individual beam particle. As will be shown below, the energy loss of the whole beam is incoherent, because it is proportional to N , the total number of beam particles in the beam rather than N^2 . [6, 7, 8]

In the time domain, each particle induces an image pulse of rms width (Exercise 1.4)

$$\sigma_\tau = \frac{b}{\sqrt{2}\gamma\beta c} \quad (1.76)$$

in the wall of the beam pipe, where b is the radius of the beam pipe in the cylindrical approximation. Suppose for simplicity that all particles have the same revolution period T_0 . If the n th particle induces an image pulse current $i_n(t) = i_0(t - t_n)$, where $t = t_n$ is the arrival time of the particle at a particular point of the ring ($0 \leq t_n < T_0$), the total image current on the beam pipe

becomes

$$I(t) = \sum_{n=1}^N i_n(t) - i_{dc}. \quad (1.77)$$

In above, i_{dc} denotes the dc component of the beam and its subtraction reflects its inability to induce image current. In the frequency domain, the spectrum of the image current is,

$$\tilde{I}(\omega) = \begin{cases} 0 & \omega = 0, \\ \sum_{n=1}^N \tilde{i}_n(\omega) & \omega \neq 0, \end{cases} \quad (1.78)$$

where $\tilde{i}_n(\omega) = \tilde{i}_0(\omega)e^{-i\omega t_n}$ and [9]

$$\tilde{i}_0(\omega) = \frac{1}{2\pi} \int_{-\infty}^{\infty} i_0(t)e^{-i\omega t} dt = -\frac{e}{2\pi I_0(x)} \quad (1.79)$$

is the Fourier transform of $i_0(t)$, with e being the particle charge, $I_0(x)$ being the modified Bessel function of order zero, and $x = \sqrt{2}\sigma_\tau\omega$ (Exercise 1.4).

It is clear that

$$\langle \tilde{I}(\omega) \rangle = 0, \quad (1.80)$$

because a perfect coasting beam should not have any nonzero frequency component. However, the expectation of the square is nonvanishing. Actually, we have

$$\langle |\tilde{I}(\omega)|^2 \rangle = \sum_{n=1}^N \langle |\tilde{i}_n(\omega)|^2 \rangle = N |\tilde{i}_0(\omega)|^2. \quad (1.81)$$

The parasitic mode gain per particle per turn is therefore

$$\overline{\Delta\mathcal{E}} = -2\pi \int_{-\infty}^{\infty} |\tilde{i}_0(\omega)|^2 \operatorname{Re} Z_0^{\parallel}(\omega) d\omega = -\frac{e^2}{\pi} \int_0^{\infty} \frac{\operatorname{Re} Z_0^{\parallel}(\omega)}{I_0(x)^2} d\omega. \quad (1.82)$$

When there is a small spread in revolution frequency in the beam particles, Eq. (1.82) gives the mean energy loss per particle per turn. The presence of the impedance perturbs the image pulse $i_0(t)$ of the single particle and alters its frequency distribution $\tilde{i}_0(\omega)$. However, this effect is of higher order and is therefore neglected in Eq. (1.82).

We notice that first, the parasitic mode loss is a single-particle effect that a particle is affected only by its own wake, and second, the parasitic mode loss receives contribution from very high frequencies because of the tiny size

of the image pulse. The single-particle effect of this problem has been verified experimentally at the CERN ISR, where the energy loss of coasting beams at 31.4 GeV/c with intensity varying for almost four orders of magnitude, from 4 mA to 32 A, was monitored and the per particle loss was found to be practically the same.

Let us take the Fermilab Recycler Ring as an illustration. It has an elliptic beam pipe of major and minor diameters 3.806" and 1.75". If we take the average and let $b = 3.528$ cm be the radius of the effective cylindrical approximate, the image pulse of a beam particle has the rms length $\sigma_\tau = 8.78$ ps (2.62 mm)[†] according to Eq. (1.76), and its rms frequency spread is $1/(2\pi\sigma_\tau) = 18.11$ GHz. Thus the knowledge of the coupling impedance up to several tens GHz will be required. It is extremely difficult to compute the coupling impedance up to these frequencies, because every variation of the vacuum chamber of the size of a millimeter has to be taken into account.

Lots of theoretical work have been performed to understand the behavior of the coupling impedance at high frequencies. It has been concluded that if the vacuum chamber is not composed of periodic cavities, the impedance at high frequencies comes mostly from the variation in cross section of the vacuum chamber. Then, the diffraction model should apply and coupling impedance Z_0^{\parallel} should roll off as $1/\sqrt{\omega}$ at high frequencies. [10] Experimental verification has been made at the CERN ISR by monitoring the energy loss of a coasting beam with its momentum centered at 3.6 GeV/c, 15.4 GeV/c, and 31.4 GeV/c. [11]

As a result, it appears to be reasonable to introduce a simple impedance model for the accelerator ring: in addition to the resistive wall impedance, there is a real part of the impedance which has a constant $Z_0^{\parallel}/n = (Z/n)_c$ below the cutoff frequency of $f_c = \omega_c/(2\pi) = 2.405c/(2\pi b)$, which amounts to 3.25 GHz

[†]One may raise the following paradox: For a beam of the Recycler Ring of intensity 0.876×10^{11} , there are on the average 6.91×10^4 particles within one rms image-pulse length ($\sigma_\tau = 8.78$ ps or 2.62 mm). The image pulse of each particle, after deducting the dc part, will be composed of waves $\exp[i\pi s/R - i\omega(t - t_0)]$ going around the ring. For these 6.91×10^4 particles that are clustered within the 2.62 mm, their waves will add up coherently for wavelength longer than 2.62 mm, because their times of arrival (or phases) t_0 will differ by less than 8.78 ps, in the same way as the occurrence of coherent synchrotron radiation in wavelengths longer than the bunch length. The solution to the paradox is simple. The waves moving around the ring in a particular frequency are generated not only by the 6.91×10^4 particles clustered within the 2.62 mm. If we look at the waves of a particular frequency at a particular location around the ring, we will be seeing in total 0.876×10^{11} waves generated by all the 0.876×10^{11} particles in the coasting beam. Since these 0.876×10^{11} particles have completely random phases, these waves tend to cancel each other, which is just Eq. (1.80). The only component that can add up to a nonzero value is the dc component, which is not present in the image current. The situation in coherent synchrotron radiation is quite different. Only those particles inside the short bunch contribute.

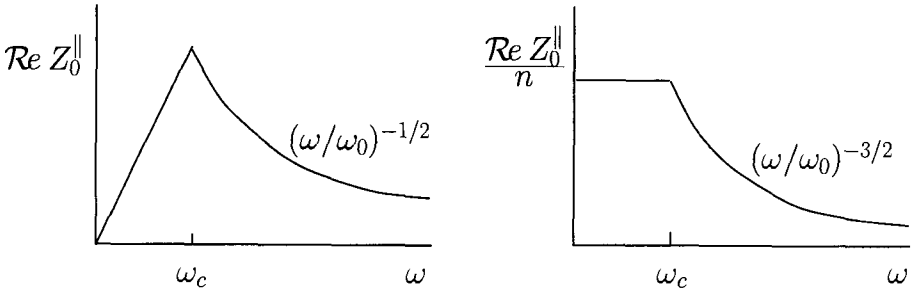


Fig. 1.7 Schematic drawing of the simplest impedance model to be used in the estimation of parasitic mode loss, showing the $\omega^{-1/2}$ asymptotic behavior of $\text{Re } Z_0^{\parallel}$ at high frequencies and constant $\text{Re } Z_0^{\parallel}/n$ below cutoff frequency.

for the Recycler Ring, and the impedance rolls off as $1/\sqrt{\omega}$ above cutoff as illustrated in Fig. 1.7, i.e., $\text{Re } Z_0^{\parallel}/n = (Z/n)_c(\omega_c/\omega)^{3/2}$ when $\omega > \omega_c$.

Monitoring the per particle energy loss of a coasting beam can reveal the impedance of accelerator ring, specially at high frequencies. As energy is lost, the beam spiral inwards resulting in an increase in revolution frequency. Thus, by monitoring the change in revolution frequency, the energy loss can be inferred from the momentum-compaction factor of the ring (see Sec. 2.1.1). Usually this change in revolution frequency is small because the energy loss is small. The energy loss due to synchrotron radiation can be easily separated because it can be computed rather accurately from the lattice of the ring and is usually very small for most hadron rings. The energy loss due to interaction with residual gas can be big or small depending on whether the residual-gas pressure in the vacuum chamber is high or low. If the beam starts off with a symmetric distribution in revolution frequency, interaction with residual gas will result in an asymmetric distribution which is calculable when the gas species and gas pressure is known. [12, 13, 14] On the other hand, interaction with wake fields will only shifts the whole distribution in revolution frequency to lower frequencies. This difference provides a way to separate the parasitic energy loss from the energy loss due to residual gas, so that the coupling impedance of the vacuum chamber can be derived. An example is shown in Fig. 1.8 for a coasting beam consisting of 0.088×10^{11} protons in the Fermilab Recycler Ring. The beam intensity was chosen to be extremely low so that increase in beam emittances and energy spread would not be significant during the long duration when distribution in revolution frequency was monitored. The left plot shows the frequency distribution at start recorded by a 1.75-GHz Schottky detector. The plot on the right shows the distribution

becoming asymmetric after 46 min. Careful separation of the effects of parasitic loss and loss due to residual gas gives a shift in revolution frequency by 0.024 Hz out of the nominal revolution frequency of 89813 Hz. This corresponds to a per particle parasitic energy loss of 0.36 MeV per hour or 1.5 meV per revolution turn.

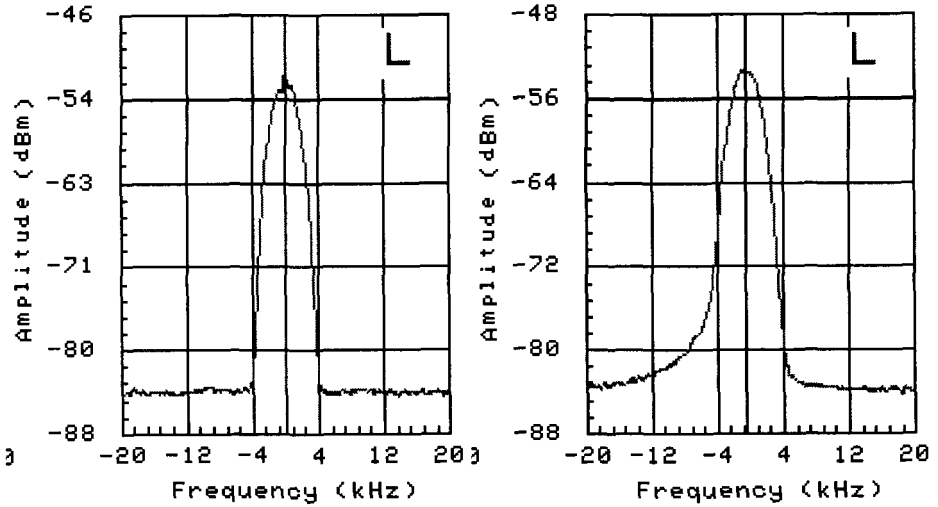


Fig. 1.8 Digitized 1.75 GHz Schottky signals at the low intensity of 0.088×10^{11} protons. Comparison of the center of the initial signal at 11.41 (left) and the peak of the final signal at 12:27 (right) gives a shift of the revolution frequency of 0.024 Hz or 0.031 Hz per hour.

1.4 Exercises

- 1.1 Prove the properties of the impedances in Eqs. (1.47)–(1.50).
- 1.2 Using a RLC -parallel circuit, derive the longitudinal impedance in Eq. (1.56) by identifying $R_{0s} = R$, $\omega_r = 1/\sqrt{LC}$, and $Q = R\sqrt{C/L}$. Then show that the wake function is $W'_0 = 0$ for $z < 0$ and

$$W'_0(z) = \frac{\omega_r R_{0s}}{Q} e^{-\alpha z/v} \left[\cos \frac{\bar{\omega} z}{v} - \frac{\alpha}{\bar{\omega}} \sin \frac{\bar{\omega} z}{v} \right], \tag{1.83}$$

for $z > 0$ with $\alpha = \omega_r/(2Q)$ and $\bar{\omega} = \sqrt{\omega_r^2 - \alpha^2}$. Similarly, show that

$$W_1(z) = -\frac{R_{1s} v \omega_r}{Q \bar{\omega}_r} e^{-\alpha z/v} \sin \frac{\bar{\omega} z}{v}, \tag{1.84}$$

for $z > 0$ and zero otherwise.

- 1.3 Show that the wake functions corresponding to the longitudinal resistive wall impedance of Eq. (1.58) and the transverse resistive wall impedance of Eq. (1.60) for a length L are, respectively,

$$W'_0(z) = -\frac{\beta^{3/2}cL}{4\pi b z^{3/2}} \sqrt{\frac{Z_0\mu_r}{\pi\sigma_c}}, \quad (1.85)$$

$$W_1(z) = -\frac{\beta^{3/2}cL}{\pi b^3 z^{1/2}} \sqrt{\frac{Z_0\mu_r}{\pi\sigma_c}}, \quad (1.86)$$

where b is the beam pipe radius, σ_c is the conductivity and μ_r the relative magnetic permeability of the beam pipe walls. The above are only approximates and are valid for $b\chi^{1/3} \ll z \ll b/\chi$, where $\chi = 1/(b\sigma_c Z_0)$. When $z \ll b\chi^{1/3}$, $W'_0(z)$ should have the proper positive sign.

- 1.4 Fill in all the missing steps in the derivation of Eq. (1.79) outlined below. [9]
 (1) Consider a point particle carrying charge e at position $r = a$ and $\theta = \theta_0$ moving with velocity v longitudinally inside a cylindrical beam pipe of radius $r = b$. The charged density is

$$\begin{aligned} \rho(r, \theta, s, t) &= \frac{e}{a} \delta(s - vt) \delta(r - a) \delta(\theta - \theta_0) \\ &= \sum_{m=0}^{\infty} \int d\omega \rho_m \delta(r - a) \cos m(\theta - \theta_0) e^{-i\omega(t-s/v)}, \end{aligned} \quad (1.87)$$

with

$$\rho_m = \frac{e}{2\pi^2 a v (1 + \delta_{m0})}. \quad (1.88)$$

- (2) In a frame at rest with the charged particle under the Lorentz transformation

$$s^* = \gamma(s - vt) \quad \text{with} \quad \gamma = \frac{1}{\sqrt{1 - v^2/c^2}}, \quad (1.89)$$

the charge density becomes static and is given by

$$\rho^*(r, \theta, s^*) = \frac{\rho(r, \theta, s, t)}{\gamma} = \sum_{m=0}^{\infty} \int d\omega \rho_m^* \delta(r - a) \cos m(\theta - \theta_0) e^{-i\omega s^*/(\gamma v)}, \quad (1.90)$$

with

$$\rho_m^* = \frac{\rho_m}{\gamma} = \frac{e}{2\pi^2 a \gamma v (1 + \delta_{m0})}. \quad (1.91)$$

We have marked all the variables in the frame at rest with the charge particle with an asterisk.

(3) In this frame at rest with the charged particle, the electrostatic potential $\phi^*(r, \theta, s^*)$ satisfies the Poisson's equation

$$\nabla^{*2}\phi^*(r, \theta, s^*) = -\frac{\rho^*(r, \theta, s^*)}{\epsilon_0}. \quad (1.92)$$

Expand the potential according to

$$\phi^*(r, \theta, s^*) = \sum_{m=0}^{\infty} \int d\omega \phi_m^*(r) \cos m(\theta - \theta_0) e^{-i\omega s^*/(\gamma v)}, \quad (1.93)$$

and the Poisson equation reduces to

$$\left[\frac{1}{r} \frac{\partial}{\partial r} \left(r \frac{\partial}{\partial r} \right) - \left(\frac{m^2}{r^2} + \frac{\omega^2}{\gamma^2 v^2} \right) \right] \phi_m^*(r) = -\frac{\rho_m^*}{\epsilon_0} \delta(r - a). \quad (1.94)$$

(4) For perfectly conducting beam-pipe walls, the solution is

$$\phi_m^*(r) = \begin{cases} A_m [I_m(xr/b)K_m(x) - K_m(xr/b)I_m(x)] & a < r < b, \\ A'_m I_m(xr/b)K_m(x) & 0 < r < a, \end{cases} \quad (1.95)$$

where $x = \omega b/(\gamma v)$, and I_m and K_m are, respectively, the modified Bessel function and Hankel function of order m . Continuity of $E_z^*(r, \theta, s^*) = -\partial\phi^*(r, \theta, s^*)/\partial s^*$ at $r = a$ gives

$$\frac{A'_m}{A_m} = 1 - \frac{K_m(xa/b)I_m(x)}{I_m(xa/b)K_m(x)}. \quad (1.96)$$

By encircling the charge distribution inside a thin shell at $a_- < r < a_+$ and $0_- < s^* < 0_+$, the divergence theorem leads to

$$A_m = -\frac{e}{2\pi^2 e \epsilon_0 \gamma v (1 + \delta_{m0})} \frac{I_m(xa/b)}{I_m(x)}. \quad (1.97)$$

(5) The radial electric field at the wall of the beam pipe is

$$E_r^*(b, \theta, s^*) = -\frac{\partial}{\partial r} \phi(r, \theta, s^*) \Big|_{r=b} = -\sum_{m=0}^{\infty} \int d\omega \frac{A_m}{b} \cos m(\theta - \theta_0) e^{i\omega s^*/(\gamma v)}, \quad (1.98)$$

and the surface charge density at the wall of the beam pipe is

$$\sigma^*(\theta, s^*) = -\epsilon_0 E_r^*(b, \theta, s^*). \quad (1.99)$$

We are not interested in the image charge distribution as a function of θ . We thus transform back to the laboratory frame and integrate over θ to arrive at the linear image charge density,

$$\bar{\lambda}(s, t) = - \int d\omega e^{-i\omega(t-s/v)} \frac{eI_m(xa/b)}{2\pi v I_0(x)}, \quad (1.100)$$

where only the monopole ($m = 0$) contributes. We next transform the variable to arrival time $\tau = t - s/v$ and obtain the linear image charge density

$$\lambda(\tau) = - \int d\omega e^{-i\omega\tau} \frac{e}{2\pi I_0(x)}, \quad (1.101)$$

which is normalized to the particle image charge when integrated over τ . We have also moved the beam towards the axis of the beam pipe ($a \rightarrow 0$) so that $I_m(xa/b)$ disappears from the numerator.

(6) The rms spread of the distribution can be obtained by performing the integration

$$\sigma_\tau^2 = \int d\tau \int d\omega e^{-i\omega\tau} \frac{\tau^2}{2\pi I_0(x)}, \quad (1.102)$$

which can be rewritten as

$$\sigma_\tau^2 = - \int d\tau \int d\omega e^{-i\omega\tau} \frac{d^2}{d\omega^2} \left[\frac{1}{2\pi I_0(x)} \right], \quad (1.103)$$

and can be evaluated easily because the integration over τ just gives the Dirac δ -function.

1.5 Appendix: A Collection of Wakes and Impedances

Below is a collection of coupling impedances and wake functions for various elements of the vacuum chamber. These are taken from Sec. 3.2.5 of *Handbook of Accelerator Physics and Engineering*, edited by A. W. Chao and M. Tigner, World Scientific, 1998. [4] All known errors and typos have been corrected. The first expression concerning wall resistivity on the next page has been generalized so that it is valid even when the frequency approaches zero. The relative permeability μ_r of the wall of the beam pipe has also been included.

3.2.5 Explicit Expressions of Impedances and Wake Functions

K. Y. Ng, FNAL

General Remarks and Notations:		
<p>W'_m denotes mth azimuthal longitudinal wake function as a function of distance z for $z < 0$. When $z > 0$, $W'_m(z) = 0$ and $W'_m(0) = \lim_{z \rightarrow 0^-} W'_m(z)$. Similar for transverse wake W_m.</p> <p>The mth azimuthal longitudinal impedance $Z_m^{\parallel}(\omega) = \int e^{-i\omega z/v} W_m^{\parallel}(z) dz/v$ is related to the transverse impedance of the same azimuthal $Z_m^{\perp}(\omega) = \int e^{-i\omega z/v} W_m^{\perp}(z) idz/(\beta v)$ by $Z_m^{\parallel} = (\omega/c) Z_m^{\perp}$ (valid when $m \neq 0$). In many cases, $\beta = v/c$ has been set to 1.</p> <p>Unless otherwise stated, round beam pipe of radius b is assumed. $C = 2\pi R$ is the ring circumference and n is the revolution harmonic. $Z_0 \approx 377 \Omega$ is the free-space impedance. ϵ_0 and μ_0 are the free-space dielectric constant and magnetic permeability.</p>		
Description	Impedances	Wakes
Space-charge: [1] beam radius a in a length L of perfectly conducting beam pipe of radius b .	$\frac{Z_0^{\parallel}}{n} = i \frac{Z_0 L}{2C\beta\gamma^2} \left[1 + 2 \ln \frac{b}{a} \right]$ $Z_{m \neq 0}^{\perp} = i \frac{Z_0 L}{2\pi\beta^2\gamma^2 m} \left[\frac{1}{a^{2m}} - \frac{1}{b^{2m}} \right]$	$W'_0 = \frac{Z_0 c L}{4\pi\gamma^2} \left[1 + 2 \ln \frac{b}{a} \right] \delta'(z)$ $W_{m \neq 0} = \frac{Z_0 c L}{2\pi\gamma^2 m} \left[\frac{1}{a^{2m}} - \frac{1}{b^{2m}} \right] \delta(z)$
Resistive Wall: [1] pipe length L , wall thickness t , conductivity σ_c , skin depth δ_{skin} .	$\frac{Z_m^{\parallel}}{L} = \frac{\omega}{c} \frac{Z_m^{\perp}}{L} = \frac{Z_0 c / (\pi b^{2m})}{[1 + \text{sgn}(\omega)i](1 + \delta_{m0})bc \sqrt{\frac{\sigma_c Z_0 c}{2 \omega } - \frac{ib^2\omega}{m+1} + \frac{imc^2}{\omega}}}$ $t \gg \delta_{\text{skin}} = \sqrt{2c/(\omega Z_0\sigma_c)}, \quad \omega \gg c\chi/b, \quad \chi = 1/(Z_0\sigma_c b)$	
For $t \gg \delta_{\text{skin}}$ and $b/\chi \gg z \approx c/ \omega \gg b\chi^{1/3}$.	$Z_m^{\parallel} = \frac{\omega}{c} Z_m^{\perp}$ $Z_m^{\parallel} = \frac{1 - \text{sgn}(\omega)i}{1 + \delta_{0m}} \frac{L}{\pi\sigma_c \delta_{\text{skin}} b^{2m+1}}$	$W_m = -\frac{c}{\pi b^{2m+1}(1 + \delta_{m0})} \sqrt{\frac{Z_0}{\pi\sigma_c}} \frac{L}{ z ^{1/2}}$ $W'_m = -\frac{c}{2\pi b^{2m+1}(1 + \delta_{m0})} \sqrt{\frac{Z_0}{\pi\sigma_c}} \frac{L}{ z ^{3/2}}$
For $t \ll \delta_{\text{skin}}$ or very low freq., and $b/\chi \gg z \approx c/ \omega \gg \sqrt{bt}$.	$\frac{Z_0^{\parallel}}{L} = -\frac{iZ_0 t \omega}{2\pi bc}, \quad \frac{Z_1^{\perp}}{L} = -\frac{iZ_0 t}{\pi b^3}$	$\frac{W'_0}{L} = -\frac{Z_0 t c}{2\pi b} \delta'(z), \quad \frac{W_1}{L} = -\frac{Z_0 t c}{\pi b^3} \delta(z)$
A pair of strip-line BPM's: [2] length L , angle each subtending to pipe axis ϕ_0 , forming transmission lines of characteristic impedance Z_c with pipe.	$Z_0^{\parallel} = 2Z_c \left[\frac{\phi_0}{2\pi} \right]^2 \left[2 \sin^2 \frac{\omega L}{c} - i \sin \frac{2\omega L}{c} \right]$ $Z_1^{\perp} = \left[\frac{Z_0^{\parallel}}{\omega} \right]_{\text{pair}} \frac{c}{b^2} \left[\frac{4}{\phi_0} \right]^2 \sin^2 \frac{\phi_0}{2}$	$W'_0 = 2Z_c c \left[\frac{\phi_0}{2\pi} \right]^2 [\delta(z) - \delta(z+2L)]$ $W_1 = \frac{8Z_c c}{\pi^2 b^2} \sin^2 \frac{\phi_0}{2} [H(z) - H(z+2L)]$
The strip-lines are assumed to terminate with impedance Z_c at the upstream end.		
Heifets inductive impedance: [3] low freq. pure inductance \mathcal{L} . Z_0^{\parallel} rolls off as $\omega^{-1/2}$.	$Z_0^{\parallel} = -\frac{i\omega\mathcal{L}}{(1 - i\omega a/c)^{3/2}}$ $\rightarrow -i\omega\mathcal{L} \text{ as } a \rightarrow 0$	$W'_0 = \frac{c^2 \mathcal{L}}{a\sqrt{\pi a z}} \left[1 + \frac{2z}{a} \right] e^{z/a}$ $\rightarrow c^2 \mathcal{L} \delta'(z) \text{ as } a \rightarrow 0$
Pill-box cavity at low freq.: length g , radial depth $h + b$, where $g \leq h \ll b$. [6]	$Z_0^{\parallel} = -i \frac{\omega Z_0}{2\pi cb} \left[gh - \frac{g^2}{2\pi} \right]$ $Z_1^{\perp} = -i \frac{Z_0}{\pi b^3} \left[gh - \frac{g^2}{2\pi} \right]$	$W'_0 = -\frac{Z_0 c}{2\pi b} \left[gh - \frac{g^2}{2\pi} \right] \delta'(z)$ $W_1 = -\frac{Z_0 c}{\pi b^3} \left[gh - \frac{g^2}{2\pi} \right] \delta(z)$

Description	Impedances	Wakes
<p>Pill-box cavity at low freq.: length g, radial depth $h + b$, where $h \ll g \ll b$. [6]</p>	$Z_0^{\parallel} = -i \frac{\omega Z_0 h^2}{\pi^2 c b} \left[\ln \frac{2\pi g}{h} + \frac{1}{2} \right]$ $Z_1^{\perp} = -i \frac{2Z_0 h^2}{\pi^2 b^3} \left[\ln \frac{2\pi g}{h} + \frac{1}{2} \right]$	$W_0' = -\frac{Z_0 c h^2}{\pi^2 b} \left[\ln \frac{2\pi g}{h} + \frac{1}{2} \right] \delta'(z)$ $W_1 = -\frac{2Z_0 c h^2}{\pi^2 b^3} \left[\ln \frac{2\pi g}{h} + \frac{1}{2} \right] \delta(z)$
<p>Pill-box cavity: length g, radial depth d. At freq. $\omega \gg c/b$, diffraction model applies. [1]</p>	$Z_m^{\parallel} = \frac{[1 + \text{sgn}(\omega)i]Z_0}{(1 + \delta_{m0})\pi^{3/2}b^{2m+1}} \sqrt{\frac{cg}{ \omega }}$ $Z_m^{\perp} = \frac{\omega}{c} Z_m^{\parallel}$	$W_m = -\frac{2Z_0 c \sqrt{2g}}{(1 + \delta_{m0})\pi^2 b^{2m+1}} z ^{1/2}$ $W_m' = \frac{Z_0 c \sqrt{2g}}{(1 + \delta_{m0})\pi^2 b^{2m+1}} z ^{-1/2}$
<p>Optical model: [7] A series of cavities of periodic length L. Each cavity has width g, high Q resonances of freq. $\omega_n/(2\pi)$ and loss factor $k_n^{(m)}$ for azimuthal mode m.</p> <p>Formulas for computation of W_m'. $\text{erfc}(x)$ is the complementary error function.</p>	$\text{Re}Z_m^{\parallel} = \sum_{n=1}^N \pi k_n^{(m)} \delta(\omega - \omega_n) + \frac{2\pi C_{sv} G(\bar{\nu}) F(\nu)}{(1 + \delta_{m0})b^{2m}} H(\omega - \omega_N)$ $W_m' = \sum_{n=1}^N 2k_n^{(m)} \cos \frac{\omega_n z}{c} + \frac{2C_{sv} G(\bar{\nu})}{(1 + \delta_{m0})b^{2m}} \int_{\omega_N}^{\infty} d\omega F(\nu) \cos \frac{\omega z}{c}$ <p>where $C_{sv} = 2Z_0 j_{m1}^2 / (\pi^2 \zeta^2 \beta) \approx 650 \Omega$ for $m = 0$ and 1650Ω for $m = 1$, j_{m1} is first zero of Bessel function J_m, $\zeta = 0.8237$.</p> $G(\bar{\nu}) = \bar{\nu}^2 K_1^2(\bar{\nu}), \quad F(\nu) = \frac{\sqrt{\bar{\nu} + 1}}{(\nu + 2\sqrt{\bar{\nu} + 2})^2}, \quad \bar{\nu} = \frac{\omega b}{\beta \gamma c}, \quad \nu = \frac{\omega}{\omega_{sv}} = \frac{4b^2 \omega}{\zeta^2 c \sqrt{g} L}$ $\int_{\bar{\omega}}^{\infty} d\omega F(\nu) \cos \frac{\omega z}{c} = \omega_{sv} \bar{F}_0(z/c) - \int_0^{\bar{\omega}} d\omega F(\nu) \cos \frac{\omega z}{c}$ $\bar{F}_0(x) = \int_0^{\infty} d\omega F(\nu) \cos \omega x = \frac{\pi}{4} (1 + 4x) e^{2x} \text{erfc}(\sqrt{2x}) - \sqrt{\frac{\pi x}{2}}$	
<p>Resonator model for the mth azimuthal, with shunt imp. $R_s^{(m)}$, resonant freq. $\omega_r/(2\pi)$, quality factor Q. [1]</p>	$Z_m^{\parallel} = \frac{R_s^{(m)}}{1 + iQ(\omega_r/\omega - \omega/\omega_r)}$ $Z_m^{\perp} = \frac{c}{\omega} \frac{R_s^{(m)}}{1 + iQ(\omega_r/\omega - \omega/\omega_r)}$	$W_m = \frac{R_s^{(m)} c \omega_r}{Q \bar{\omega}_r} e^{\alpha z/c} \sin \frac{\bar{\omega}_r z}{c}$ <p>where $\alpha = \omega_r/(2Q)$</p> $\bar{\omega}_r = \sqrt{ \omega_r^2 - \alpha^2 }$
<p>Res. freq. $\omega_{mnp}/(2\pi)$ and shunt impedance $(R_s)_{mnp}$ of a pill-box cavity for nth radial and pth longitudinal modes. Radial depth d and length g. x_{mn} is nth zero of Bessel function J_m. [8]</p>	$\frac{\omega_{mnp}^2}{c^2} = \frac{x_{mn}^2}{d^2} + \frac{p^2 \pi^2}{g^2}$ $\left[\frac{R_s}{Q} \right]_{0np} = \frac{Z_0}{x_{0n}^2 J_0^2(x_{0n})} \frac{8c}{\pi g \omega_{0np}} \begin{cases} \sin^2 \frac{g\omega_{0np}}{2\beta c} \times \frac{1}{1 + \delta_{0p}} & p \text{ even} \\ \cos^2 \frac{g\omega_{0np}}{2\beta c} & p \text{ odd} \end{cases}$ $\left[\frac{R_s}{Q} \right]_{1np} = \frac{Z_0}{J_1^2(x_{1n})} \frac{2c^2}{\pi g d^2 \omega_{1np}^2} \begin{cases} \sin^2 \frac{g\omega_{1np}}{2\beta c} & p \neq 1 \text{ and even} \\ \cos^2 \frac{g\omega_{1np}}{2\beta c} & p \text{ odd} \end{cases}$	

Description	Impedances	Wakes
Low-freq. response of a pill-box cavity: [4] length g , radial depth d . When $g \gg 2(d-b)$, replace g by $(d-b)$. Here, $S = d/b$. [5]	$\frac{Z_0^{\parallel}}{n} = -i \frac{Z_0 g}{2\pi R} \ln S$ $Z_1^{\perp} = -i \frac{Z_0 g}{\pi b^2} \frac{S^2 - 1}{S^2 + 1}$	$W_0' = -\frac{Z_0 c g}{2\pi} \ln S \delta'(z)$ $W_1 = -\frac{Z_0 c g}{\pi b^2} \frac{S^2 - 1}{S^2 + 1} \delta(z)$
	Effect will be one half for a step in the beam pipe from radius b to radius d , or vice versa, when $g \gg 2(d-b)$.	
Iris of half elliptical cross section at low freq.: width $2a$, maximum protruding length h . [5]	$Z_0^{\parallel} = -i \frac{\omega Z_0 h^2}{4cb}$ $Z_1^{\perp} = -i \frac{Z_0 h^2}{2b^3}$	$W_0' = -\frac{Z_0 c h^2}{4b} \delta'(z)$ $W_1 = -\frac{Z_0 c h^2}{2b^3} \delta(z)$
Pipe transition at low freq.: tapering angle θ , transition height h . γ is Euler's constant and ψ is the psi-function. [6]	$Z_0^{\parallel} = \frac{\omega b^2 Z_1^{\perp}}{2c} = -i \frac{\omega Z_0 h^2}{2\pi^2 c b} \left\{ \ln \left[\frac{b\theta}{h} - 2\theta \cot \theta \right] + \frac{3}{2} - \gamma - \psi \left(\frac{\theta}{\pi} \right) - \frac{\pi}{2} \cot \theta - \frac{\pi}{2\theta} \right\}$ $W_0' = - \left \frac{Z_0^{\parallel}}{\omega} \right c^2 \delta'(z), \quad W_1 = - \left Z_1^{\perp} \right c \delta(z), \quad h \cot \theta \ll b$	
Pipe transition at low frequencies with transition height $h \ll b$. [6]	$Z_0^{\parallel} = \frac{\omega b^2}{2c} Z_1^{\perp} = -i \frac{\omega Z_0 h^2}{2\pi^2 c b} \left(\ln \frac{2\pi b}{h} + \frac{1}{2} \right)$ $W_0' = - \left \frac{Z_0^{\parallel}}{\omega} \right c^2 \delta'(z), \quad W_1 = - \left Z_1^{\perp} \right c \delta(z)$	
Kicker with window-frame magnet: [9] width a , height b , length L , beam offset x_0 horizontally, and all image current carried by conducting current plates.	$Z_0^{\parallel} = \frac{\omega^2 \mu_0^2 L^2 x_0^2}{4a^2 Z_k}$ $Z_1^{\perp} = \frac{c \omega \mu_0^2 L^2}{4a^2 Z_k}$	$W_0' = -\frac{c^3 \mu_0^2 L^2 x_0^2}{4a^2 Z_k} \delta_0''(z)$ $W_1 = -\frac{c^3 \mu_0^2 L^2}{4a^2 Z_k} \delta'(z)$
	$Z_k = -i\omega\mathcal{L} + Z_g$ with $\mathcal{L} \approx \mu_0 bL/a$ the inductance of the windings and Z_g the impedance of the generator and the cable. If the kicker is of C-type magnet, x_0 in Z_0^{\parallel} should be replaced by $(x_0 + b)$.	
Traveling-wave kicker with characteristic impedance Z_c for the cable, and a window magnet of width a , height b , and length L . [9]	$Z_0^{\parallel} = \frac{Z_c}{4} \left[2 \sin^2 \frac{\theta}{2} - i(\theta - \sin \theta) \right], \quad Z_1^{\perp} = \frac{Z_c L}{4ab} \left[\frac{1 - \cos \theta}{\theta} - i \left(1 - \frac{\sin \theta}{\theta} \right) \right]$ $W_0' = \frac{Z_c c}{4} \left[\delta(z) - \delta \left(z - \frac{Lc}{v} \right) - \frac{Lc}{v} \delta'(z) \right]$ $W_1 = \frac{Z_c v}{4ab} \left[H(z) - H \left(z - \frac{Lc}{v} \right) - \frac{Lc}{v} \delta(z) \right]$	
	$\theta = \omega L/v$ denotes the electrical length of the kicker windings and $v = Z_c a c / (Z_0 b)$ is the matched transmission-line phase velocity of the capacitance-loaded windings.	
Bethe's electric and magnetic moments of a hole of radius a in beam pipe wall. [10]	Electric and magnetic dipole moments when wavelength $\gg a$: \vec{E} and \vec{B} are electric and magnetic flux density at hole when hole is absent. This is a diffraction solution for a thin-wall pipe.	$\vec{d} = -\frac{2\epsilon_0}{3} a^3 \vec{E}, \quad \vec{m} = -\frac{4}{3\mu_0} a^3 \vec{B}$

Description	Impedances	Wakes
<p>Small obstacle [5, 11] on beam pipe, size \ll pipe radius, freq. below cutoff. α_e and α_m are electric polarizability and magnetic susceptibility of the obstacle.</p>	$Z_0^{\parallel} = -i \frac{\omega Z_0}{c} \frac{\alpha_e + \alpha_m}{4\pi^2 b^2}$ $Z_1^{\perp} = -i \frac{Z_0(\alpha_e + \alpha_m)}{\pi^2 b^4} \cos \Delta\varphi$	$W'_0 = -Z_0 c \frac{\alpha_e + \alpha_m}{4\pi^2 b^2} \delta'(z)$ $W_1 = -Z_0 c \frac{\alpha_e + \alpha_m}{\pi^2 b^4} \cos \Delta\varphi \delta(z)$
<p>$\Delta\varphi$ is the azimuthal angle between the obstacle and the direction concerning Z_1^{\perp} and W_1.</p>		
<p>Polarizabilities for various geometry: beam pipe radius is b and wall thickness is t.</p>		
<p>Elliptical hole: major and minor radii are a and d. $K(m)$ and $E(m)$ are complete elliptical functions of the first and second kind, with $m = 1 - m_1$ and $m_1 = (d/a)^2$. For long ellipse \perp beam, major axis $a \ll b$, beam pipe radius, because the curvature of the beam pipe has been neglected here. [12]</p>	$\alpha_e + \alpha_m = \begin{cases} \frac{\pi a^3 m_1^2 [K(m) - E(m)]}{3E(m)[E(m) - m_1 K(m)]} & \xrightarrow{m \rightarrow 1} \\ \frac{\pi a^3 [E(m) - m_1 K(m)]}{3[K(m) - E(m)]} & \text{long ellipse} \end{cases}$ $\alpha_e + \alpha_m \xrightarrow{m \rightarrow 0} \frac{\text{circular}}{3} \frac{2a^3}{3} \quad \text{circular hole } a = d \ll b$ <p>Above are for $t \ll a$, $\times 0.56$ (circular) or $\times 0.59$ (long ellipse) when $t \geq a$.</p> <p>For higher frequency correction, add to $\alpha_e + \alpha_m$ the extra term,</p> $+ \frac{2\pi a^3}{3} \left[\frac{11\omega^2 a^2}{30c^2} \right] \text{circular, } \begin{cases} \left[-\frac{\pi a d^2}{3} \left[\frac{\omega^2 a^2}{5c^2} \right] \right] & \parallel \text{ beam} \\ \left[+\frac{2\pi a^3}{3} \left[\frac{2\omega^2 a^2}{5c^2 [\ln(4a/d) - 1]} \right] \right] & \perp \text{ beam} \end{cases}$	$\begin{cases} \frac{\pi d^4 [\ln(4a/d) - 1]}{3a} & \parallel \text{ beam} \\ \frac{\pi a^3}{3 [\ln(4a/d) - 1]} & \perp \text{ beam} \end{cases} \quad \begin{matrix} d \ll b \\ a \ll b \end{matrix}$
<p>Rectangular slot: length L, width w.</p>	$\alpha_e + \alpha_m = w^3(0.1814 - 0.0344w/L) \quad t \ll a, \quad \times 0.59 \text{ when } t \geq a$	
<p>Rounded-end slot: length L, width w.</p>	$\alpha_e + \alpha_m = w^3(0.1334 - 0.0500w/L) \quad t \ll a, \quad \times 0.59 \text{ when } t \geq a$	
<p>Annular-ring-shaped cut: inner and outer radii a and $d = a + w$ with $w \ll d$.</p>	$\alpha_e + \alpha_m = \frac{\pi^2 d^2 a}{2 \ln(32d/w) - 4} - \frac{\pi^2 w^2 (a + d)}{16} \quad t \ll d$ $\alpha_e + \alpha_m = \pi d^2 w - \frac{1}{2} w^2 (a + d) \quad t \geq d$	
<p>Half ellipsoidal protrusion with semi axes h radially, a longitudinally, and d azimuthally. ${}_2F_1$ is the hypergeometric function.</p>	$\alpha_e + \alpha_m = 2\pi a h d \left[\frac{1}{b} + \frac{1}{I_c - 3} \right]$ $I_b = {}_2F_1\left(1, 1; \frac{5}{2}; 1 - \frac{h^2}{a^2}\right), \quad I_c = {}_2F_1\left(1, \frac{1}{2}; \frac{5}{2}; 1 - \frac{a^2}{h^2}\right), \quad \text{if } a = d$ $\alpha_e + \alpha_m = \pi a^3 \quad \text{if } a = d = h, \quad \frac{2\pi h^3}{3[\ln(2h/a) - 1]} \quad \text{if } a = d \ll h$ $\alpha_e + \alpha_m = \frac{8h^3}{3} \left[1 + \left(\frac{4}{\pi} - \frac{\pi}{4} \right) \frac{a}{h} \right] \quad \text{if } a \ll h = d$ $\alpha_e + \alpha_m = \frac{8\pi h^4}{3a} \left[\ln \frac{2a}{h} - 1 \right] \quad \text{if } a \gg h = d$	

<p>Array of pill-boxes, box spacing L, each with gap width g, beam pipe radius b. Gluckstern-Yokoya-Bane formula [15] at high freq. to order $(kg)^{-1}$:</p>	<p>For each cavity of length L with $k = \omega/c$,</p> $Z_0^{\parallel} = \frac{iZ_0L}{\pi kb^2} \left\{ 1 + [1 + i \operatorname{sgn}(k)] \frac{\alpha L}{b} \sqrt{\frac{\pi}{ k g}} \right\}^{-1}$ <p>with $k = \omega/c$. $\alpha = 1$ when $g/L \ll 1$ and $\alpha = \alpha_1 = 0.4648$ when $g/L = 1$, the limiting case of infinitely thin irises. In general, with $\Upsilon = g/L$, $\alpha(\Upsilon) = 1 - \alpha_1 \Upsilon^{1/2} - (1 - 2\alpha_1)\Upsilon + \mathcal{O}(\Upsilon^{3/2})$.</p>
<p>The above pill-box array with radial depth d generates a single-frequency resonance impedance at $\omega_r = c \left(\frac{2L}{bgd} \right)^{1/2}$. [16, 17]</p>	$Z_0^{\parallel} = \frac{Z_0cL}{2\pi b^2} \sum_{\omega' = \pm\omega_r} \left[\pi \delta(\omega - \omega') + \frac{i}{\omega - \omega'} \right]$ $Z_1^{\perp} = \frac{2cL}{b^2\omega} Z_0^{\parallel}$ $W_0'(z) = \frac{Z_0cL}{\pi b^2} \cos \frac{\omega_r z}{c}$ $W_1(z) = \frac{2Z_0L}{\pi b^4\omega_r} \sin \frac{\omega_r z}{c}$ <p>The corresponding resonator per pill box has $\frac{R_s^{(0)}\omega_r}{Q} = \frac{Z_0cL}{\pi b^2}$.</p>
<p>Smooth toroidal b and $R = \frac{1}{2}(a + b)$. As the Lorentz factor $\gamma \rightarrow \infty$, (ultra-relativistic beam), a <u>curvature contribution</u> remains for the longitudinal impedance. [18]</p>	<p>Valid from zero frequency up to just below synchronous resonant modes, i.e., $0 < \nu < \sqrt{R/h}$ with $\nu = \omega h/c$,</p> $\frac{Z_0^{\parallel}}{n} = iZ_0 \left(\frac{h}{\pi R} \right)^2 \left\{ \left[1 - e^{-2\pi(b-R)/h} - e^{-2\pi(R-a)/h} \right] \left[1 - 3 \left(\frac{\nu}{\pi} \right)^2 \right] + 0.05179 - 0.01355 \left(\frac{\nu}{\pi} \right)^2 \right\} + \rho$ $\approx iZ_0 \left(\frac{h}{\pi R} \right)^2 \left[A - 3B \left(\frac{\nu}{\pi} \right)^2 \right]$ <p>where ρ is quadratic in ν. As $(b-a)/h$ increases, ρ vanishes exponentially and $A \approx B \approx 1$. In general, $A/B \approx 1$ implying $\operatorname{Im} Z_0^{\parallel}$ changes sign (a node) near $\nu = \pi/\sqrt{3}$.</p>
<p>Rf cage: beam of radius a surrounded by a cylindrical cage or array of N wires of radius ρ_w, length L at radial distance r_w from beam center. Wire filling factor is $f_w = N\rho_w/(\pi r_w)$. Formulas are valid at low frequencies, $0 < n < R/r_w$ and $N \gg 1$.</p>	$\frac{Z_0^{\parallel}}{n} = \frac{iZ_0L}{4\pi R\beta\gamma^2} \left[1 + 2\ln \frac{r_w}{a} + C_{\parallel} \right], \quad Z_1^{\perp} = \frac{iZ_0L}{2\pi\beta^2\gamma^2} \left[\frac{1}{a^2} - \frac{1 - C_{\perp}}{r_w^2} \right]$ <p>Without metallic beam pipe outside wire array or cage, [19]</p> $C_{\parallel} = -\frac{2\ln(nr_w/R)\ln(\pi f_w)}{N\ln(nr_w/R) + \ln(\pi f_w)}, \quad C_{\perp} = -\frac{2\ln(\pi f_w)}{N - 2\ln(\pi f_w)}$ <p>With infinitely conducting metallic beam pipe, radius $b > r_w$, [20]</p> $C_{\parallel} = 2\ln \frac{b}{r_w} - \frac{2N[\ln(b/r_w)]^2}{N\ln(b/r_w) - \ln(\pi f_w) + \ln[1 - (r_w/b)^{2N}]}$ $C_{\perp} = \frac{[1 - (r_w/b)^2][(r_w/b)^2 + (b/r_w)^2]\{\ln[1 - (r_w/b)^{2N}] - 2\ln(\pi f_w)\}}{N[1 - (r_w/b)^2] + [(r_w/b)^2 + (b/r_w)^2]\ln[1 - (r_w/b)^{2N}] - 2\ln(\pi f_w)}$ <p>A ceramic layer between the wires and metallic beam pipe has negligible effect on the impedances.</p>

<p>Wall roughness [13] 1-D axisymmetric bump, $h(z)$ or 2-D bump $h(z, \theta)$. Valid for low frequency <math>k = \omega/c \ll (\text{bump length or width})^{-1}</math>, $h \ll b$, pipe radius, and $\nabla h \ll 1$.</p>	<p>1-D: $Z_0^{\parallel} = -\frac{2ikZ_0}{b} \int_0^{\infty} \kappa \tilde{h}(\kappa) ^2 d\kappa$ with spectrum $\tilde{h}(k) = \frac{1}{2\pi} \int_{-\infty}^{\infty} h(z) e^{-ikz} dz$ 2-D: $Z_0^{\parallel} = -\frac{4ikZ_0}{b} \sum_{m=-\infty}^{\infty} \int_{-\infty}^{\infty} \frac{\kappa^2}{\sqrt{\kappa^2 + m^2/b^2}} \tilde{h}_m(\kappa) ^2 d\kappa$ with spectrum $\tilde{h}_m(k) = \frac{1}{(2\pi)^2} \int_0^{2\pi} d\theta \int_{-\infty}^{\infty} dz h(z, \theta) e^{-ikz - im\theta}$</p>
Heifets and Kheifets formulas for tapered steps and tapered cavity at high frequencies. [14]	
<p>Taper in from radius h to b ($< h$), out from radius b to h; tapering angle α. Tapering inefficient for a bunch of rms length σ, if $2(h-b)\tan\alpha \gg$ σ. All formulas here and below are valid for <i>positive</i> $k = \omega/c$ only.</p>	<p>$\text{Re}Z_0^{\parallel} = \pm \frac{Z_0}{2\pi} \ln \frac{h}{b} + (Z_0^{\parallel})_{\text{step}}$, $\text{Re}Z_1^{\perp} = \pm \frac{Z_0 b}{4\pi} \left(\frac{1}{b^2} - \frac{1}{h^2} \right) + (Z_1^{\perp})_{\text{step}} \begin{cases} + \text{in} \\ - \text{out} \end{cases}$ $(Z_0^{\parallel})_{\text{step}} = \frac{Z_0}{2\pi} \ln \frac{h}{b}$, $\tan\alpha > \frac{h-b}{kb^2}$, $(Z_0^{\parallel})_{\text{step}} = \frac{Z_0}{4} kb \tan\alpha$, $\tan\alpha \ll \frac{1}{kb}$ $(Z_1^{\perp})_{\text{step}} = \frac{Z_0}{4\pi b} \left[1 - \frac{1}{(1+kb)^2} {}_2F_1\left(1, \frac{3}{2}, 3, \frac{4bh}{(b+h)^2}\right) \right]$, $\tan\alpha > \frac{h-b}{kb^2}$, $kb \gg 1$ $(Z_1^{\perp})_{\text{step}} = \frac{Z_0 b}{4\pi} \left(\frac{1}{b^2} - \frac{1}{h^2} \right)$, $\tan\alpha > \frac{h-b}{kb^2}$, $kb \gg 1$, $h \gg b$ $(Z_1^{\perp})_{\text{step}} = \frac{Z_0}{16b} (kb)^3 \tan\alpha$, $\tan\alpha \ll \frac{1}{kb}$</p>

References

- [1] A. W. Chao, *Physics of Collective Beam Instabilities in High Energy Accelerators*, (Wiley, 1993), ch.2.
- [2] K. Y. Ng, *Part. Accel.* **23**, 93 (1988).
- [3] S.A. Heifets, G. Sabbi, SLAC/AP-104 (1996).
- [4] E. Keil, B. Zotter, *Part. Accel.* **3**, 11 (1972); K. Y. Ng, Fermilab Report FN-389 (1981).
- [5] S. S. Kurennoy, *Phys. Rev.* **E55**, 3529 (1997); S. S. Kurennoy, R. L. Gluckstern, *Phys. Rev.* **E55**, 3533 (1997).
- [6] S. S. Kurennoy, G. V. Stupakov, *Part. Accel.* **45**, 95 (1994).
- [7] A. M. Sessler, unpublished citation in E. Keil, *Nucl. Instr. Method* **100**, 419 (1972); L. A. Veinshtein, *Sov. Phys. JETP* **17**, 709 (1963); D. Brandt, B. Zotter, CERN-ISR/TH/82-13 (1982)
- [8] C. C. Johnson, *Field and Wave Electrodynamics*, (McGraw-Hill), Ch.6.
- [9] G. Nassibian, F. Sacherer, *Nucl. Instr. Method* **59**, 21 (1971); G. Nassibian, CERN/PS 84-25 (BR) (1984); CERN 85-68 (BR) (1986).
- [10] M. Sands, SLAC note PEP-253 (1977); H.A. Bethe, *Phys. Rev.* **66**, 163 (1944).
- [11] S. S. Kurennoy, *Part. Accel.* **39**, 1 (1992); *Part. Accel.* **50**, (1995) 167; R. L. Gluckstern, *Phys. Rev.* **A46**, 1106, 1110 (1992); S. S. Kurennoy, R. L. Gluckstern, G. V. Stupakov, *Phys. Rev.* **E52**, 4354 (1995).
- [12] A. Fedotov, PhD Thesis, U. Maryland (1997)
- [13] R. Gluckstern, *Phys. Rev.* **D39**, 2773, 2780 (1989); G. Stupakov, PAC 95 3303, K. Yokoya and K. Bane, PAC 99, p.1725.
- [14] A. Novokhatski, A. Mosnier, PAC 97, p.1661.
- [15] K. L. F. Bane, A. Novokhatski, SLAC Report AP-117 (1999).
- [16] K. Y. Ng and R. Warnock, PAC 89, p.798, *Phys. Rev.* **D40**, 231 (1989).
- [17] T. S. Wang, AIP Conf. Proc. 448, 286 (1998).
- [18] T. S. Wang and R. Gluckstern, PAC 99, p.2876.
- [19] G. V. Stupakov, SLAC-PUB-7908 (1998), *Phys. Rev. ST AB* **1**, 064401 (1998).
- [20] S. A. Heifets, *Phys. Rev.* **D40**, 3097 (1989); S. A. Heifets, S. A. Kheifets, *Rev. Mod. Phys.* **63**, 631 (1990).